Machine Learning
Data Analytics

Friedrich-Alexander-Universität
Technische Fakultät

EmpkinS

Extraction of Pre-Ejection Period as Marker for Acute Psychosocial Stress from Wearable Sensors and Interferometry Radar

Master's Thesis in Medical Engineering

submitted
by

Ulla Sternemann

born 23.12.1996 in München

Written at

Machine Learning and Data Analytics Lab
Department Artificial Intelligence in Biomedical Engineering
Friedrich-Alexander-Universität Erlangen-Nürnberg (FAU)

in Cooperation with

Chair of Health Psychology (FAU)
Institute of High-Frequency Technology, Hamburg University of Technology (TUHH)

Advisors: Robert Richer M.Sc., Arne Küderle M.Sc., Prof. Dr. Bjoern Eskofier (FAU)
Nils Albrecht M.Sc., Prof. Dr. Alexander Kölpin (TUHH)
Prof. Dr. Nicolas Rohleder (Chair of Health Psychology, FAU)

Started: 15.09.2022

Finished: 17.04.2023

Ich versichere, dass ich die Arbeit ohne fremde Hilfe und ohne Benutzung anderer als der angegebenen Quellen angefertigt habe und dass die Arbeit in gleicher oder ähnlicher Form noch keiner anderen Prüfungsbehörde vorgelegen hat und von dieser als Teil einer Prüfungsleistung angenommen wurde. Alle Ausführungen, die wörtlich oder sinngemäß übernommen wurden, sind als solche gekennzeichnet.
Die Richtlinien des Lehrstuhls für Bachelor- und Masterarbeiten habe ich gelesen und anerkannt, insbesondere die Regelung des Nutzungsrechts.

Erlangen, den 17.04.2023

Übersicht

Stress ist allgegenwärtig im täglichen Leben der meisten Menschen. Die Reaktion des menschlichen Körpers auf akuten psychosozialen Stress wird hauptsächlich durch das sympathische Nervensystem (SNS) und die Hypothalamus-Hypophysen-Nebennierenrinden-Achse reguliert. Diese Stressreaktion wird meist anhand von Biomarkern wie Cortisol und α-amylase bewertet, die im Blut- oder Speichel gemessen werden. Jedoch sind diese Messmethoden arbeitsintensiv, teuer und erlauben keine kontinuierliche Erfassung der Stressreaktion.

Ein neuer Ansatz für einfachere Erfassung der Stressreaktion ist die sogenannte Präejektionsperiode (PEP). Die PEP beschreibt die Dauer zwischen dem Einsetzen der ventrikulären Depolarisation und der Öffnung der Aortenklappe. Mehrere Studien haben bewiesen, dass sich die PEP bei erhöhter SNS-Aktivität verkürzt. Dementsprechend wird die PEP als Indikator für SNS-Aktivität und für akuten Stress angesehen. Die Goldstandardmethode um die PEP zu erfassen erfordert die gleichzeitige Aufzeichnung eines Elektrokardiogramms (EKG) und eines Impedanzkardiogramms (ICG) und ist dementsprechend nur im Labor durchführbar. Deswegen wird in dieser Arbeit untersucht, ob die PEP alternativ mithilfe von kabellos aufgezeichneten Seismokardiographie und EKG Daten erfasst werden kann. Dazu wurde eine Studie mit zweiundzwanzig Teilnehmern durchgeführt, die verschiedene stressinduzierende und -reduzierende Aufgaben durchführten. Währenddessen wurden EKG-, ICG-, SCG-, und Interferometrie-Radar-Daten aufgezeichnet. Anschließend wurden mehrere Algorithmen für die Extraktion der PEP entwickelt.

Die erzielten Ergebnisse zeigten, dass die nicht möglich war die PEP basierend auf den Daten der tragbaren Sensoren innerhalb jedes Herzschlags präzise zu erfassen, weil die tragbaren Sensoren aufgrund ihrer geringen Abtastrate nicht in der Lage waren, den physiologisch relevanten Bereich PEP ausreichend genau zu erfassen. Der mittlere Fehler für die kabellos erfassten PEP Werte betrug 29,9 %, was bei einem durchschnittlichen Referenzwert von 138,3 ms etwa 41,4 ms entspricht. Allerdings ermöglichten die entwickelten Algorithmen es, die verschiedenen stressauslösenden und stressreduzierenden Aufgaben basierend auf den kabellos erfassten Sensordaten anhand der durschnittlichen gemessenen PEP Werte zu unterscheiden. Zukünftig könnte eine kontinuierliche unkomplizierte Erfassung der PEP zusätzlich verbessert werden, indem man die SCG-Sensoren durch Interferometrie-Radar ersetzt.

Abstract

Stress has become a pervasive phenomenon in most people's daily lives. Despite being a healthy physiological response of the human body, excessive stress can severely impact physical and mental health. The human body's reaction to acute psychosocial stress is mainly modulated by the sympathetic nervous system (SNS) and the hypothalamic-pituitary-adrenal axis. This stress response is usually assessed based on blood and saliva biomarkers, such as cortisol and α-amylase. To date, these methods provided a relatively good measure of the effects of stress on the body and, thus, on health. However, these established measures are labor-intensive, expensive, and do not allow continuous assessment of the stress response.

A promising approach towards less obtrusive stress assessment might be the so-called pre-ejection period (PEP). The PEP, which is a short systolic time interval, is defined as the duration between the onset of ventricular depolarization and the aortic valve opening (AO). Several studies proved that the PEP shortens with increased sympathetic activity. Accordingly, PEP can be considered a suitable marker for SNS activity and, thus, acute stress. The gold standard approach for PEP measurement requires simultaneous recording of the electrocardiogram (ECG) and impedance cardiography (ICG) signals and, therefore, is only applicable in laboratory settings. Hence, this thesis explores whether PEP assessment based on wirelessly recorded seismocardiogram (SCG) and ECG is feasible. Therefore, a study including twenty-two participants was conducted. The participants performed several stress-inducing and -reducing tasks while ECG, ICG, SCG, and interferometry radar data was recorded. An algorithm for reference PEP extraction, as well as for wearable sensor-based PEP extraction, was implemented.

The obtained results highlight that beat-to-beat PEP assessment was not feasible with the utilized sensors since the wearable sensors were not able to capture the physiologically relevant range of the PEP sufficiently accurately due to their low sampling rate. The mean error for wirelessly acquired PEP was 29.9 %, which corresponds to 41.4 ms for an average reference PEP of 138.3 ms. However, instead of beat-to-beat PEP assessment, the developed wearable sensor-based PEP extraction algorithms allow distinguishing the stress-inducing and the stress-reducing tasks according to the average captured PEP. In the future, continuous and unobtrusive PEP assessment might be further improved by replacing SCG sensors with interferometry radar.

Contents

Chapter 1

Introduction

Stress has become a pervasive phenomenon in most people's daily lives. Despite being a healthy physiological response of the human body, excessive stress can severely impact both physical and mental health [OCo21]. Consequently, stress is increasingly acknowledged as a leading contributor to various chronic diseases in many countries around the world [OCo21; APA19].

From a physiological point of view, the human body reacts to acute psychosocial stress by triggering specific neuroendocrine responses, which are mainly modulated by two main stress response pathways: the sympathetic nervous system (SNS) and the hypothalamic-pituitary-adrenal (HPA) axis [Ulr09]. Activation of the HPA axis due to stress provokes the secretion of cortisol into the bloodstream and the saliva. Accordingly, cortisol serves as a well-characterized and specific marker for HPA axis activation [Fol10]. Additionally, activation of the SNS initiates the immediate "fight-or-flight" response via the release of epinephrine, leading to increased heart rate (HR) and cardiac contraction force, as well as the secretion of salivary α-amylase (sAA) [McC16; Can53]. A common approach for assessment of the human stress response is by measuring these neuroendocrine markers using saliva samples. However, this requires considerable effort on the researchers' side while also being obtrusive for the participant [Gra19] and consequently interferes at least to some extent with natural human behavior [Kaz79]. Furthermore, the use of saliva samples allows neither continuous nor real-time quantization of the stress response, as saliva samples can be taken at most every few minutes, and concentration changes of the respective biomarkers occur only with certain delays [Gra19; Fol10].

To overcome these issues, the literature often proposes using heart rate variability (HRV) as a surrogate marker for SNS activity and, therefore, as a potential indicator of psychosocial stress. This approach offers the advantage that HRV is an easy-to-obtain and non-invasive electrophysiological parameter and, in addition, can be recorded continuously over extended time periods. However, the heart rate is modulated by both branches of the autonomic nervous system, the SNS and the parasympathetic nervous system (PNS), which can both influence the HRV separately [Kim18]. Consequently, the HRV, which is in fact controlled primarily by parasympathetic withdrawal rather than sympathetic activation, has limitations regarding its suitability for assessing the body's stress response [Kim18; Rey13; Ber94].

Another promising marker for sympathetic activity and, thus, for psychosocial stress, might be the so-called PEP. In the literature on unobtrusive stress assessment methods, the suitability of PEP as novel stress marker has been investigated increasingly in recent years [Dro22; Rah18; Bri14]. The PEP is a short systolic time interval within the cardiac cycle and is defined as the time period between the onset of the electrical activity of the heart and the corresponding mechanical activity. Accordingly, the start of the PEP is defined as the onset of ventricular depolarization, whereas the PEP end is defined as the beginning of left ventricular blood ejection [New79]. The results of several studies investigating the relationship between SNS and PEP by pharmacologically modulating SNS activity proved that PEP shortens with increased sympathetic activity [Dro22; Har67]. Also, PEP remains unaffected by pharmacologically induced changes in PNS activity [Cac94a]. These findings highlight that PEP can be utilized as a biomarker for acute stress since it reflects SNS activity changes [Dro22].

The gold standard approach for PEP measurement requires simultaneous recording of electrocardiogram (ECG) and impedance cardiography (ICG). The ECG signal is used to extract the PEP start point as the start of ventricular depolarization, which corresponds to the onset of the Q-wave. For extraction of the PEP end point, which is equivalent to the aortic valve opening (AO), the ICG signal is needed [Tav16]. Unfortunately, the acquisition of ICG signals is rather obtrusive and requires expensive measurement equipment. Furthermore, extracting the necessary fiducial points from both signals is not trivial, which highlights the need for novel PEP measurement methods to enable unobtrusive and continuous stress assessment [Deh19; Lie13].

For these reasons, recent research explored wearable and contactless approaches for PEP estimation. For example, wearable inertial measurement units (IMUs) were used to extract

the SCG signal from chest micro-movements. Since the AO can also be estimated from SCG signals this might be a suitable and more unobtrusive replacement for the ICG. Combined with a portable ECG device, this provides an option for wearable PEP measurement [Deh19; Sha19]. A further improvement towards unobtrusive PEP estimation might be the use of radar. Instead of attaching inertial sensors to the body, the AO can also be estimated from Doppler radar signals, which are acquired completely contactless [Don22; Wil18; Xia18].

Although researchers explored such novel PEP estimation approaches, these methods have not yet been evaluated extensively within stress-related scenarios. Hence, further research is needed to investigate the feasibility of PEP-based assessment of acute psychosocial stress [Dro22; Wei21].

The goal of this master's thesis is, therefore, to first investigate how various stress-inducing and stress-reducing tasks influence the PEP. Besides, three algorithms for different PEP estimation approaches will be implemented: the ICG-based gold standard method, a wearable sensor-based method, and a novel method based on interferometry radar and wearable ECG (ECG_W). Accordingly, the feasibility and performance of the newly developed radar-based PEP estimation approach will be evaluated. Consecutively, this novel approach will be compared to both the gold standard method and established approaches proposed in literature which utilize wearable sensors. Therefore, a dataset containing ECG, ICG, IMU, and radar data is collected while participants perform several stress-inducing and -reducing tasks. Conclusively, this work hopefully provides insights into novel, easy-to-use methods for measuring PEP and, thus, for unobtrusive assessment of psychosocial stress.

This thesis is organized as follows: Chapter 2 explains the medical and technical background necessary for this thesis. In particular, this chapter describes the physiological stress response of the human body and several biomarkers suitable for its assessment, including PEP. Chapter 3 presents relevant research in the field of wearable and contactless measurement of body signals. In Chapter 4, the data acquisition process is outlined, and the methods used for PEP estimation and evaluation of the implemented algorithms are described. The results are presented and discussed in Chapter 5, while Chapter 6 concludes the thesis by providing an outlook.

Chapter 2

Background

2.1 Pre-Ejection Period

2.1.1 Cardiac Cycle

The primary task of the human heart is to supply all vital organs with blood. Figure 2.1 provides an overview of the heart's anatomy. The heart consists of the right and the left part, each composed of an atrium and a ventricle separated by a heart valve.These atrioventricular valves are called the mitral valve in the left part of the heart and the tricuspid valve in the right part. From a functional point of view, the right and left parts of the heart form two separate pumping systems. The left part of the heart pumps oxygenated blood through the aortic valve into the aorta. Then, the blood flows into the systemic circulation of the body. Within the right system, deoxygenated blood transported to the heart through the inferior and superior vena cava is pumped through the pulmonary valve into the pulmonary artery, which leads to the lungs. The blood is oxygenated in the lungs and subsequently flows back to the left part of the heart through the pulmonary vein. In each cardiac cycle, the heart undergoes a phase of contraction followed by relaxation, referred to as systole and diastole, respectively. During the diastole, the ventricles fill with blood, and during the systole, the blood is ejected again [Mic19; Opi04; Mil90].

Due to the mechanical activity of the heart, each heartbeat causes small vibrations, which build two distinct heart sounds. These sounds are usually audible with a stethoscope and visible in a phonocardiogram (PCG) signal. Both heart sounds are linked to specific events within the cardiac cycle. The first heart sound S1 occurs at the beginning of ventricular systole

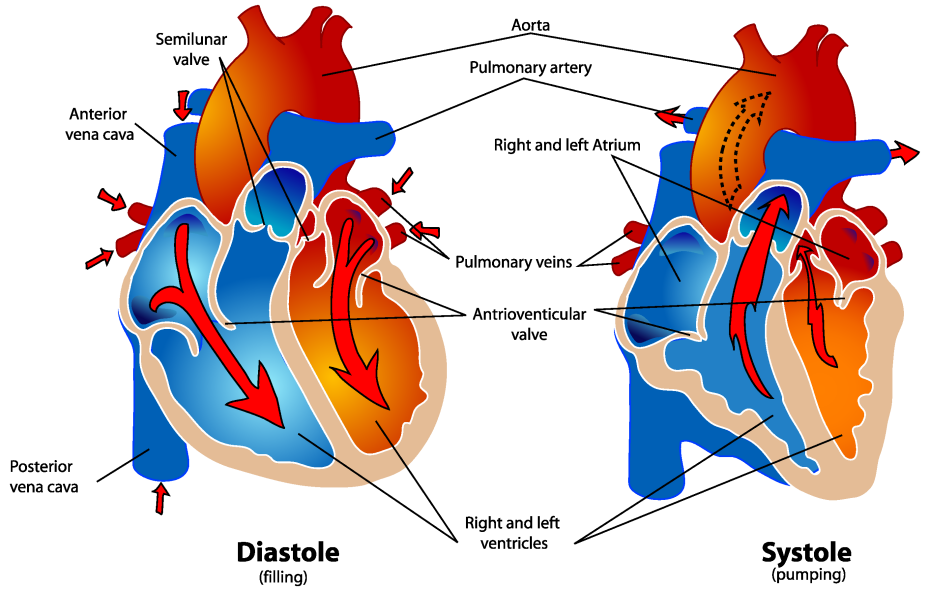

Figure 2.1: Schematic illustration of the human heart anatomy and the blood flow during the cardiac cycle [Opb18]

and is generated by the closing of the mitral and tricuspid valves. The second heart sound originates from the closing of the aortic and pulmonary valves and hence marks the end of the systole [Mil90].

The rhythmic contraction and relaxation phases of the atria and ventricles are regulated by electrical signals generated and transmitted by the heart's conduction system. These electrical signals arise in the sinoatrial node, which is a collection of specialized cells located at the right atrium. Subsequently, the signal spreads through the atria, the atrioventricular node (AV node), and the bundle of His. The bundle of His splits into two branches transmitting the electric signal via the Purkinje fibers to the left and the right ventricle, where it finally triggers ventricular contraction. This coordinated sequence of electrical impulses ensures that the heart beats in a synchronized manner [Opi04].

The transmission of the above-described electrical signal can be measured with electrocardiography and and correspondingly is visualized as an electrocardiogram (ECG). An exemplary ECG signal of a physiological heartbeat is depicted in Figure 2.2. The spread of the electric impulse through the atria is represented by the P-wave. The subsequent spike, referred to as the QRS complex, reflects the rapid ventricular depolarization, whereby the Q-wave corresponds to the electric impulse spreading through the ventricular septum. The

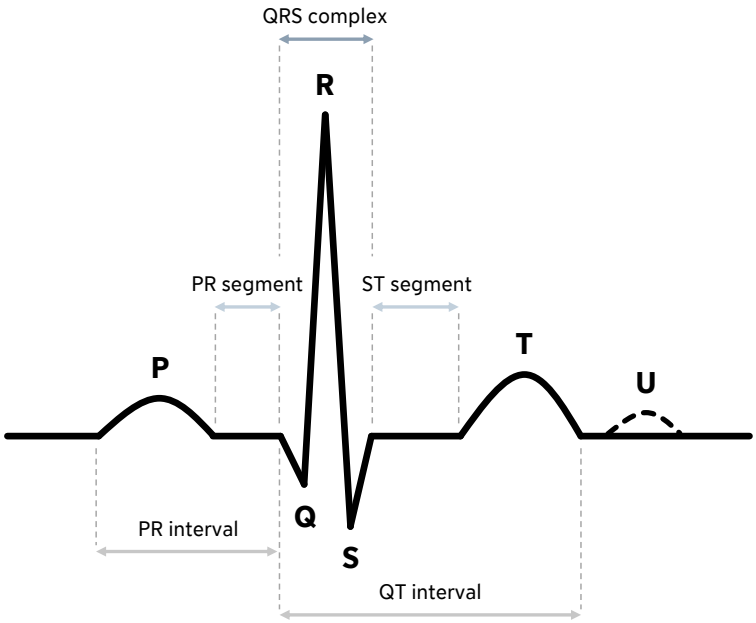

Figure 2.2: Schematic illustration of an ECG of a heart in normal sinus rhythm (modified from [Atk09]) according to Einthoven's lead II [Ein08]

last component of the electrocardiographic trace, the T-wave, represents the repolarization of the myocardium. Sometimes, also the U-wave is visible, which is an additional wave occurring after the T-wave. It is thought to be linked to delayed repolarization of the Purkinje fibers, yet it is often indiscernible due to its low amplitude [Opi04].

2.1.2 Physiology of the Pre-Ejection Period

The literature defines several time intervals within the cardiac cycle. In particular, systolic time intervals, like left ventricular ejection time (LVET), total electromechanical systole (QS_2), and pre-ejection period (PEP), are often utilized in clinical practice to assess left ventricular performance in a non-invasive way. Abnormalities in systolic time intervals typically indicate the presence of myocardial diseases, coronary artery disease, or arterial hypertension. Furthermore, the severity of such conditions can be assessed based on these parameters [Bou90; Wei77].

The PEP is defined as the time interval between the onset of ventricular depolarization and the onset of left ventricular blood ejection. Accordingly, the PEP's start corresponds

to the Q-wave onset in the ECG, whereas the PEP's end is equivalent to the aortic valve opening (AO) [New79; Wei77].

From a physiological point of view, the PEP is comprised of two distinct components: the electromechanical delay and the isovolumetric contraction (IVC) [Tav16; Kro17]. The electromechanical delay, which corresponds to the duration between the depolarization onset and the beginning of ventricular contraction, occurs because the electrical signal needs to be transmitted from the AV node throughout the entire ventricular myocardium. During the IVC, intraventricular pressure rises until it exceeds the aortic pressure causing the aortic valve to open and blood to be ejected [Opi04; Mil90]. Accordingly, variation in PEP could theoretically occur due to variation in one or both of these components. However, the electromechanical delay is presumed to be fairly constant (around 30 – 40 ms in healthy humans) since it remains largely unaffected by most physiological and pathophysiological states, except in the case of a left bundle branch block [Lew77]. Consequently, changes in the PEP are probably caused by varying duration of the IVC. The IVC, and thus the PEP, primarily reflects cardiac contractility. However, it can besides be influenced by other cardiovascular variables like preload, which corresponds to the amount of ventricular filling, and afterload, which corresponds the systemic vascular resistance, and diastolic blood pressure. Therefore, it is important to take these variables into account as potential confounding factors when evaluating cardiac contractility based on PEP [Kro17].

Beyond that, the findings of several researchers indicate that the PEP can additionally be modulated by changes in sympathetic activity and hence by acute mental stress [Wei21; Kro17]. This will be discussed in more detail in a subsequent section of this thesis.

2.1.3 Gold Standard Pre-Ejection Period Measurement

Within clinical settings, systolic time intervals are usually assessed based on ECG and simultaneously acquired ultrasound, whereas the latter is referred to as echocardiography [Tav16; Ott13]. There are two options to obtain the timing of AO via echocardiography, either by using the motion mode (M-mode), or by Doppler echocardiography. The M-mode is able to capture rapid intracardiac motion, such as AO, since it records movements of the examined tissue with high temporal resolution. Doppler echocardiography visualizes the blood flow velocity, for instance, in the ascending aorta. Hence, AO can be detected as it corresponds to a sharp increase in blood flow in this area [Ott13]. However, determining PEP based on

echocardiography requires trained personnel to perform the labor-intensive data acquisition and analysis. Moreover, the recordings are typically performed with the patient positioned supine, which obviously limits possible application scenarios. Therefore, echocardiography is neither a suitable technique for continuous PEP assessment over longer periods of time nor for non-clinical settings [Bur13].

Besides using echocardiography, PEP measurements can be obtained from impedance cardiography (ICG) recordings in combination with synchronized ECG recordings. This method for conducting PEP measurements does not require specialized training and is applicable in a wider range of use cases, for example, for research purposes in laboratory settings. Accordingly, it is considered the gold standard approach for PEP measurement [Tav16].

As previously mentioned, the start point of the PEP is defined as the onset of ventricular depolarization and, consequently, corresponds to the onset of the Q-wave in the ECG signal. The PEP end point is defined as the aortic valve opening (AO), which can be determined from the ICG signal [Tav16; She90].

Impedance cardiography is used to assess cardiac mechanical function by measuring changes in electrical impedance caused by thoracic blood flow. The ICG's principle is based on Ohm's law (2.1), where R is the resistance, U is the voltage, and I is the current. Analogously, the impedance Z corresponds to the resistance in the case of alternating current $\widetilde{I}$ (2.2).

$$R = \frac{U}{I} \qquad (2.1) \qquad\qquad Z = \frac{U}{\widetilde{I}} \qquad (2.2)$$

The ICG device induces an alternating sinusoidal current along the thorax with a constant magnitude I into the body via electrodes. Simultaneously, the resulting voltage U is recorded via additional electrodes. The conventional method for ICG acquisition presented by Kubicek et al. required four tetrapolar band electrodes, but these are nowadays usually replaced by four disposable spot electrodes for reasons of practicality. A schematic illustration of the measurement setup is shown in Figure 2.3. As blood functions as a conductor, each heartbeat and the consecutive increase in blood flow through the aorta leads to a change in thoracic impedance Z. Since I is known and U is measured the resulting impedance change can be calculated. [Wol97; She90; Kub70]. In order to investigate systolic time intervals, the first derivative dZ/dt of the impedance signal is usually utilized since the timing of relevant cardiac events can be determined from its waveform. The point of AO, often referred to as the B-point, is equivalent to the onset of the rapid upslope in the dZ/dt signal corresponding

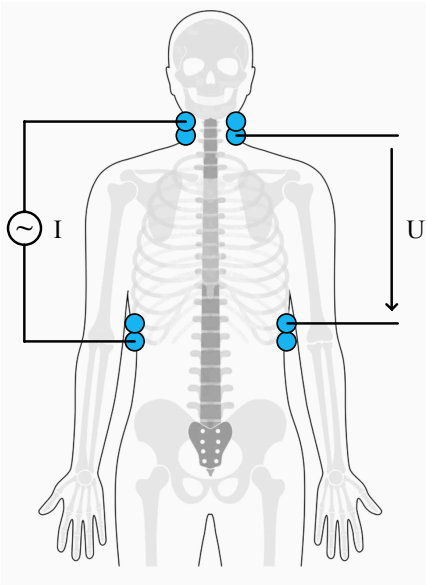

Figure 2.3: Schematic illustration of the measurement setup for ICG with induced alternating current I and measured voltage U

to the start of left ventricular blood ejection [Wol97; She90]. Finally, the PEP is the time interval between the Q-onset and the B-point detected in the ICG dZ/dt signal [She90]. An example of the PEP derived from ECG and ICG data of a couple of heartbeats can be seen in Figure 2.4.

However, it is not trivial to reliably detect the B-point and, thus, AO in a fully automated way without relying on manual corrections. To resolve this issue, the literature proposes various algorithms for improved B-point extraction, for example, utilizing the second or third derivative of the impedance signal [Árb17], using autoregressive models for subsequent refinement of detected B-point positions [For18], or using a weighted time window-based approach [Mil22]. Although such methods improve automatic B-point detection, ICG signal analysis is still not straightforward, hence making continuous PEP measurement a challenging task [Lie13]. Furthermore, measurement equipment is expensive, and the measurement itself is rather obtrusive due to the number of necessary electrodes and wires. Overall, this highlights the need for novel methods, as those might facilitate PEP assessment in a broader range of especially non-clinical application scenarios [Deh19].

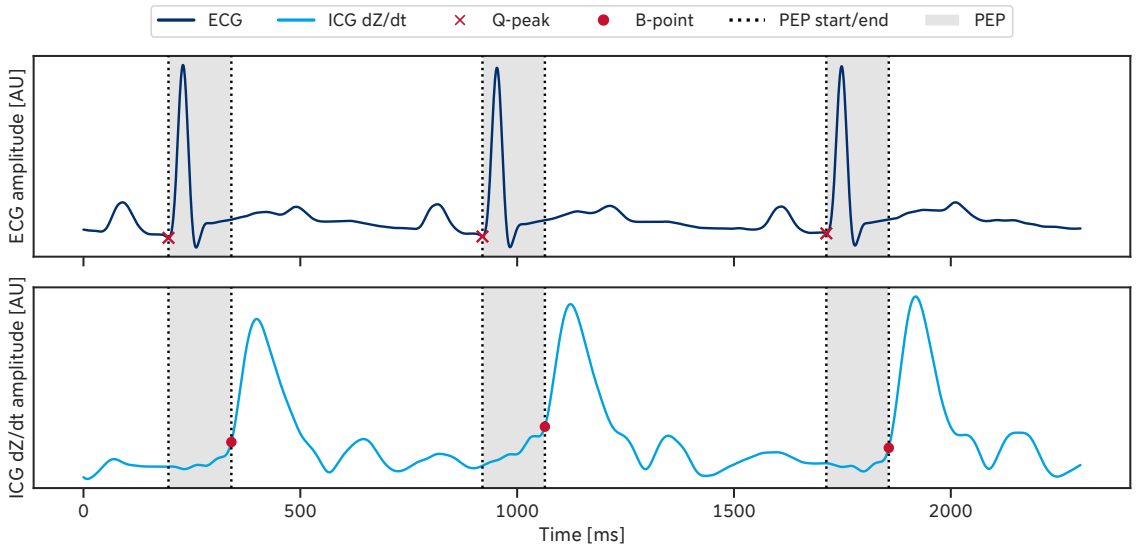

Figure 2.4: PEP extracted from ECG and ICG signals of one person over three consecutive heartbeats (with PEP start defined as Q-peak to facilitate automatic detection as proposed by [Ber04], and B-point as PEP end).

2.1.4 Seismocardiography-based Pre-Ejection Period Estimation

Attempting to develop a less obtrusive technique for measuring PEP, several researchers have proposed seismocardiography as a useful tool for assessing cardiac time intervals [Tav16]. The principle of seismocardiography was first described by Roman M. Baevsky, who intended to measure precordial movements caused by the mechanical activity of the heart. Initially, it was used to monitor the health state of astronauts onboard a spacecraft [Bae64]. To acquire a seismocardiogram (SCG) signal, an accelerometer (ACC) is attached to the chest at the lower part of the sternum, which records low-frequency vibrations caused by myocardial activity. Commonly, the dorsoventral component of the ACC signal is considered the SCG signal, however, the remaining components can also be included. The SCG's waveform consists of a systolic and a diastolic profile which both show a characteristic shape. Researchers assume that this characteristic shape results from certain cardiac events since they induce myocardial vibrations, which are transmitted through the tissue and become detectable at the chest wall. Therefore, several studies analyzed the relationship between the SCG waveform and the occurrence of cardiac events detected with echocardiography and found that certain fiducial points in the SCG are associated with the opening and closing of the aortic and mitral

valves [Sør18; Cro94]. Within the systolic part of the SCG waveform, at least in case of a clear signal, the point of AO corresponds to the peak following the first major minimum [Deh19; Tav16; Cro94].

As the timing of AO can be determined from the SCG signal, this technique provides an alternative option to ICG for detecting the PEP end point. By combining this with a wearable ECG device, PEP assessment could be conducted solely based on wearable sensing techniques [Deh19]. Figure 2.5 depicts an exemplary SCG waveform, the location of AO within it, and the resulting PEP.

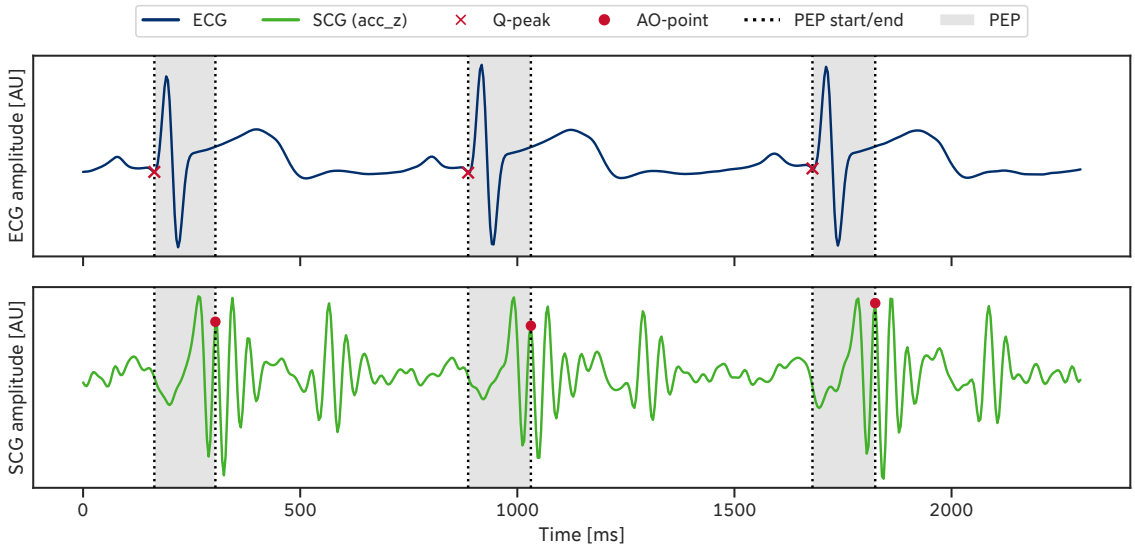

Figure 2.5: PEP extracted from ECG and SCG signals of one person over three consecutive heartbeats (with PEP start defined as Q-peak to facilitate automatic detection as proposed by [Ber04], and AO extracted from SCG as PEP end).

Accordingly, SCG-based PEP acquisition provides a portable approach for assessing PEP and thus is applicable in a wider range of settings. Additionally, nowadays, the required sensors are highly accurate while being very inexpensive. Hence, this technique is considerably more accessible than the ICG-based approach. Nevertheless, the use of the SCG also has its drawbacks. For example, automated extraction of fiducial points is not trivial because the morphology of the signal can considerably vary between individuals or due to slightly different sensor placement [Zan13].

2.2 Stress Response Assessment

The physiological response of humans to acute psychosocial stressors, as well as individual differences in this regard, is a topic researchers have been interested in for several decades. Numerous variables, ranging from basic vital signs to complex hormone release cascades, have been investigated with the aim of assessing stress-related processes in the body [Ulr09]. In this context, also the PEP is explored as a potential biomarker for acute stress [Dro22].

2.2.1 Physiology of the Human Stress Response

Stress, which is broadly defined as an actual or anticipated threat to well-being, leads to the adaption of various biological functions. This adaption is controlled by endocrine mechanisms and the autonomic nervous system (ANS). Even though the ANS consists of two branches, the SNS and the PNS, primarily the SNS regulates the stress response [All14; Ulr09; Fol10].

Regarding the endocrine reaction to stress exposure, the main pathway here is the HPA axis. Its activation results in the release of cortisol into the bloodstream. The cortisol plasma concentration starts increasing within a few minutes after the beginning of the stressor and peaks approximately ten minutes after stress cessation. These changes in cortisol levels can be captured with either blood or saliva samples [Ulr09]. Particularly saliva samples offer the possibility of a non-invasive quantification of the individual stress response. As stress-induced cortisol patterns have been studied extensively, cortisol is acknowledged as a well-characterized HPA-axis marker [Fol10].

In contrast to the relatively slow cortisol response, the SNS response to a stressor occurs immediately within seconds [Ulr09]. This reaction of the body is commonly referred to as the ”fight-or-flight” response and is characterized by, among other things, increased HR and blood pressure, increased blood flow to the skeletal muscles, release of glucose from the liver, activation of sweat glands, and the dilation of the airways. After cessation of the stressor, the body tries to regain homeostasis [Can53; McC16]. Well-established markers for SNS activity are plasma norepinephrine and epinephrine. Accordingly, assessing SNS activity based on these markers is a rather invasive approach since it requires taking blood samples [Tho12].

2.2.2 Biomarker for Autonomic vs. Sympathetic Activity

Several non-invasive approaches attempting to quantify activity changes in the SNS have been proposed in the literature. However, it is important to note that although the SNS and the PNS together comprise the ANS, they are nevertheless two anatomically and functionally distinct structures. These two branches of the ANS innervate most organ systems and tissues in the body and ensure precise regulation of their activity. Consequently, both ANS branches are crucial for maintaining homeostasis [McC07]. However, especially concerning stress-induced modulation of SNS activity, it is essential to distinguish whether a biomarker exclusively reflects SNS activity or is also influenced by vagal activity and thus should be considered an ANS marker [Kim18; Ber94; Nat09].

A marker that has been proposed as a surrogate marker for SNS activity changes, particularly in the context of stress, is sAA since it seems to reflect changes in plasma norepinephrine [Tho12]. Similarly to cortisol, sAA can be measured via saliva samples, which is considered a non-invasive method. However, it still requires disrupting the natural behavior of the person being measured, at least to some extent. Furthermore, it is neither possible to capture the sAA concentration continuously since saliva samples can only be acquired every couple of minutes nor to capture changes in real-time since sAA levels only increase with a certain delay [Gra19; Fol10]. Besides, research indicates that actually both parts of the ANS, the sympathetic and parasympathetic mechanisms, modulate the release of sAA. Moreover, the correlations between sAA and known cardiac sympathetic markers are relatively small, which leads to the assumption that sAA is not a suitable marker for SNS activity changes [Nat09].

Moreover, the literature mentions the T-wave amplitude as potentially being associated with SNS activity. However, it was found that excitation or inhibition of the SNS induced through specific medication does not consistently alter the T-wave amplitude. Consequently, the T-wave amplitude is not assumed to be a reliable parameter for sympathetic activity [Sch83; Dro22].

Another biomarker frequently mentioned in literature as an indicator of psychosocial stress is HRV, which is very easy to obtain and also non-invasive. However, the question arises whether HRV is actually a reliable parameter for indicating acute psychosocial stress. Although the heart, and thus the HRV, is mainly controlled by the ANS, the SNS and PNS branches both influence the HRV separately [Kim18]. Because of their opposing functions, it is often assumed that SNS and PNS activity are reciprocally coupled, i.e. SNS activation

inevitably leads to PNS withdrawal. In the case of orthostatic stress, this reciprocal behavior is observed: sympathetic control of the heart increases while simultaneously parasympathetic control decreases. In contrast, SNS and PNS do not necessarily act reciprocally during exposure to psychosocial stress [Ber94]. Studies involving pharmacological blockades of either sympathetic or parasympathetic innervation of the heart observed various combinations of SNS and PNS activity and withdrawal. Additionally, this differs between individuals. Hence, sympathetic and parasympathetic activity changes can occur reciprocally, coactively, or completely independently, given that the stress response of the two autonomic branches is apparently uncorrelated [Cac94a; Ber94]. Besides, research shows that the high-frequency HRV power spectrum is mainly affected by parasympathetic activity [Rey13; Ber94; Kim18; Tho19; Cac94a], while the low frequency component is modulated by both SNS and PNS [Bic17].

In accordance with these considerations, it becomes clear that HRV, which is, in fact, primarily altered by parasympathetic withdrawal, should not be utilized to make inferences about an individual's stress response [Kim18; Rey13; New79]. Consequently, current research still seems to lack a non-invasive, easily measurable biomarker that is modulated exclusively by the SNS, remains unaffected by PNS activity changes, and hence can be used to assess SNS activity changes and thus the response to psychosocial stress [Nat09].

2.2.3 Pre-Ejection Period as Biomarker for Sympathetic Activity

The PEP might be a promising solution to the above-mentioned deficiency of suitable non-invasive SNS biomarkers [Dro22; Bri14; New79].

Some researchers assume that the PEP can provide valuable insights into SNS activity. Within several studies where participants received specific medication to "artificially" modulate SNS or PNS activity, changes in PEP were also observed. Firstly, it has been repeatedly shown that pharmacologically induced stimulation of β-adrenoceptors by epinephrine or isoproterenol, which corresponds to an increase in SNS activity, leads to shortened PEP [Dro22; Har67]. Similarly, the administration of the α_2-antagonist yohimbine, which leads to an SNS activity increase as well, also results in shortened PEP [Dro22]. In contrast, PEP is prolonged by the administration of the β-antagonist metoprolol, as well as by the α_2-agonist dexmedetomidine, as both lead to sympathetic withdrawal [Cac94a; Dro22]. Furthermore, it has been observed that during blockade of parasympathetic control induced by atropine

sulfate, PEP remains unchanged [Cac94a]. The results of these studies confirm the assumption that sympathetic activity modulates PEP, i.e. PEP is shortened when SNS activity is increased, and remains unaffected by varied PNS activity. Therefore, PEP can be considered a sensitive and specific marker for SNS activity changes, which are, for example, caused by acute psychosocial stress [Cac94a; Dro22; Wei21; Bri14].

Chapter 3

Related Work

The measurement of body signals provides valuable insights into various physiological processes of the human body. Particularly, the development of measurement techniques based on wearable or contactless sensing technology is an ongoing research topic, as this enables continuous assessment of body signals while minimizing interference with people's natural behavior [The23; Nou22; Keb20; Kaz79]. Correspondingly, researchers aim to find novel and unobtrusive methods to facilitate the continuous assessment of an individual's response to acute psychosocial stress [Tho19; Kim18].

Contactless Measurement of Body Signals

In contrast to traditional or wearable sensor-based measurement approaches, contactless methods allow for a more comfortable assessment of body signals since neither electrodes nor sensors are required to be attached to the skin [Wil18]. Further advantages are that contactless approaches are more practical for long-term data collection and that movement constraints due to wires are eliminated. The literature proposes various techniques, for example, using lasers, radio frequency (RF) signals, or infrared (IR) images, to assess a wide range of body signals like motion, emotions, or vital signs [The23; Nou22; Keb20].

Adib et al. proposed a system that uses RF signals reflected off a person's body to track their location in 3D space across multiple rooms and to roughly detect movements of body parts [Adi14]. In the work of Tan et al., WiFi-based sensing was used to monitor a person's daily activities inside their home to gather health data and detect emergency situations. Therefore, they tracked whole-body motion and limb movements [Tan15]. In their research on contactless activity recognition, Maitre et al. utilized data recorded with ultra-wideband

radars to classify 15 different activities of daily life [Mai21]. Moreover, analyzing a person's gait can provide valuable insights into their health state, especially regarding the progression of neurodegenerative diseases. Botros et al. developed a system that measures distance with rotating IR lasers and enables contactless and hence less obtrusive assessment standard gait parameters [Bot21]. Li et al., who also presented a novel gait analysis approach, used a radar sensor network consisting of a frequency-modulated continuous-wave radar and three ultra-wideband pulse radars to classify various gait patterns [Li21]. Furthermore, Seifert et al. investigated contactless gait analysis using Doppler radar and were able to extract clinically relevant kinematic and spatiotemporal gait parameters from radar data. They concluded that radar-based gait analysis offers an unobtrusive and privacy-preserving method for monitoring patients in their homes [Sei21].

Besides motion-related body signals, also sleep monitoring can yield helpful information about an individual's health. Since it is relevant to keep the sensory system as unobtrusive as possible to maintain sleeping comfort and increase acceptance, contactless options are preferable here. Yue et al. proposed an RF-based system that realizes continuous monitoring of the sleep posture of patients without reducing sleeping comfort [Yue20]. Moreover, Martinez et al. developed a system for respiration monitoring during sleep based on near-IR imaging [Mar12]. Similarly, Yang et al. also researched contactless options for respiration monitoring with the aim of diagnosing Parkinson's disease and tracking its progression based on the acquired data. They extracted respiratory signals from radio waves and hence managed to assess the health status of patients in a contactless way [Yan22]. Another novel approach for unobtrusive sleep monitoring in infants was investigated by Wang et al., who managed to extract breathing and position information from white noise emitted by a smart speaker and reflected off the infant's body [Wan19].

In addition to respiratory signals, the continuous detection of other vital signs, like HR, plays a crucial role in health assessment and monitoring. In order to obtain such measurements, contactless approaches based on technologies like lasers or radar are desirable as they are relatively comfortable for the individual being measured [Keb20; Wil18].

Morbiducci et al., Koegelenberg et al., and Bai et al. showed that chest wall vibrations caused by cardiac activity could be detected with laser-based Doppler interferometry. They were able to recover the heart sounds from the recorded signals and thus estimate the HR [Koe14; Bai12; Mor07]. Such laser-based approaches provide the advantage of having a high distance resolution and focusing precisely on the desired measurement spot. However, the

laser beam needs to be reflected directly from the skin since it cannot penetrate clothing, which limits the use of this approach in non-clinical settings [Wil18].

In contrast, radar signals have the ability to penetrate through clothing and similar materials, which makes this technology applicable in a broader range of scenarios [Wil18]. For example, in palliative care, it is essential to maintain the independence and mobility of patients and, thus, their quality of life. Therefore, Shi et al. presented a contactless system that uses a six-port continuous wave radar to monitor respiration and HR. They achieved a 97.6 % correlation between the HR and respiratory curve extracted from the radar signal and the respective reference signals [Shi18]. Furthermore, as Shi et al. presented in their work, HR and HRV could be inferred from the data recorded by a 24 GHz Six-Port-based radar system and processed with a long short-term memory (LSTM) network performing heart sound segmentation. HR and HRV were detected reliably with relative errors of around 5 % [Shi21].

Through all of these contributions, it becomes clear that contactless measurement of various body signals, especially radar-based monitoring of respiration and HR, offers great potential for numerous medical use cases.

Wearable Sensing Techniques for Pre-Ejection Period Estimation

Apart from HR measurement, researchers also addressed novel approaches for estimating more sophisticated cardiac parameters, like cardiac time intervals, including PEP. Various options for wearable sensing methods for estimating cardiac timings were investigated in the scientific literature. Some these methods involved ballistocardiogram (BCG) [Ash16; Jav16] or forcecardiogram (FCG) recordings [Cen22], whereas the majority was based on PCG or SCG signals [San22].

Klum et al. presented a method for wearable PEP estimation utilizing PCG data [Klu20]. The PCG signal, which is acquired with a stethoscope and a microphone, is the recording of heart sounds and murmurs occurring due to blood flow and the opening and closure of heart valves [Deh19; Lea52]. Klum et al. stated that PEP could be roughly estimated based on PCG signals combined with simultaneously recorded ECG data. They reported a PEP estimation error of 21 % compared to the ICG-based reference [Klu20]. However, it is questionable whether the PCG is an appropriate choice to determine PEP, as the PCG signal does not actually contain any information about the timing of AO. Although the time interval between mitral valve closure (MC) and AO is very short, the first heart sound S1 in the PCG signal is

caused by MC, not by AO. Consequently, the accurate PEP end point cannot be determined from the PCG signal [Deh19; Tav16].

The most common approach for wearable PEP estimation is to extract the AO times and thus the PEP end point from SCG recordings, while the PEP start point is extracted from ECG_W. Dehkordi et al. compared the accuracy of SCG-based beat-to-beat extraction of cardiac timings, including PEP, to manually annotated multimodal echocardiography as the reference method. They exclusively used the dorsoventral component of the ACC signal to estimate PEP and reported an average error of 12.8 %. However, they suggested that these results might be improved by additionally utilizing the craniocaudal and the left-to-right component of the ACC signal, as well as rotational information from a gyroscope (GYRO) since chest wall vibrations induced by cardiac activity are not limited to only the dorsoventral direction [Deh19]. Since the SCG signal is known to show considerable variation, Ashouri et al. investigated the effects of different sensor placements on the performance of their PEP estimation model. Variations in the SCG waveform occur either when sensors are placed slightly differently or due to variations between different individuals. They obtained the best PEP results by combining the information of two sensors, one placed at the sternum and one below the left clavicle, yielding a root mean square error (RMSE) of 11.6 ± 0.4 ms compared to the ICG-based reference. Interestingly, they achieved a more accurate estimate of PEP with sensors placed below the left (RMSE = 13.4 ± 0.4 ms) or right clavicle (RMSE = 13.2 ± 0.4 ms) than with the conventional placement on the sternum (RMSE = 16.4 ± 0.7 ms) [Ash18]. Moreover, Tavakolian et al. examined SCG-based PEP and stroke volume estimation in their work. They compared their results to reference values derived from both ultrasound Doppler and ICG and concluded that PEP estimation using SCG is a promising non-invasive approach [Tav10].

Contactless Sensing Techniques for Pre-Ejection Period Estimation

Although PEP estimation can be accomplished entirely with wearable sensors, it requires attaching several sensors directly to the person's skin [Don22; Xia18]. A further step towards realizing unobtrusive PEP measurement would be to replace such sensors with contactless options wherever possible. For example, this could be achieved by capturing the timing of AO with radar-based sensing technology [Shi21; Ha20]. Correspondingly, some researchers reported using this approach for PEP assessment.

The work of Buxi et al. highlights the feasibility of radar-based PEP estimation. Their approach for estimating AO was not entirely contactless since they used a 2.45 GHz system combined with body-contact antennas. However, the acquisition of such radar signals is also possible in a contactless manner. They reported a Pearson correlation coefficient of 0.72 ($p < 0.0001$) between radar-based PEP and reference PEP measured with ECG and ICG [Bux17]. Xia et al., who investigated contactless SCG measurement via 5.8 GHz microwave Doppler radar signals, found a high morphological correlation of the second derivative of the radar displacement signal and the dorsoventral SCG signal. Furthermore, they managed to estimate AO timings with an RMSE of < 2 ms compared to the SCG-derived reference. However, the corresponding study only included 8 participants, all of whom were male. Also, their method lacks comparison with a sophisticated ground truth like ICG or echocardiography [Xia18]. Pour Ebrahim et al. measured the PEP using simultaneously recorded ECG and continuous wave radar signals. The data set they acquired included 40 participants and three different postures: sitting, standing, and supine. Even though they reported reasonable PEP values, they did not evaluate the accuracy of their radar-based approach compared to a gold standard method [Pou20]. The contribution of Dong et al. described an approach to estimate PEP solely from data acquired with a 24 GHz digital dc-tuning Doppler radar and reported an RMSE of 8.6 ms corresponding to a mean absolute percentage error of 6.35 % for estimated PEP. The presented work has some shortcomings, though. Firstly, the analyzed data were only obtained from a single person. Secondly, they defined PEP as the time between ECG Q-onset and the beginning of the rise in aortic pressure recorded with an invasive sensor, which seems reasonable since the aortic pressure rises because the aortic valve opens but nevertheless does not correspond to the standard PEP definition [Don22].

In conclusion, these findings demonstrate that PEP estimation is feasible using wearable sensors. Furthermore, combining wearable and contactless sensing technologies seems to be a promising method to measure the PEP as unobtrusive as possible. However, neither of these novel PEP estimation approaches has yet been used with the objective of assessing an individual's stress response in a continuous and real-time manner.

Chapter 4

Methods

4.1 Data Acquisition

To evaluate the performance of the wearable PEP estimation approach (SCG + ECG_W), as well as of the radar-based approach (radar + ECG_W), a study was conducted at the *Machine Learning and Data Analytics Lab*. The acquired dataset included 22 young, healthy adults. The participants were asked to perform several stress-inducing and -reducing tasks while conventional ECG, ICG, wearable ECG, SCG, and radar data were concurrently recorded. Written informed consent was obtained from all participants before testing.

4.1.1 Study Protocol

The study protocol created for this work consisted of six active phases, each lasting for three minutes, in which the participants completed different tasks. Passive baseline phases of two minutes duration were incorporated at the beginning and the end of the recording, as well as between the active phases. Accordingly, the total recording duration was 32 minutes per participant. The six active phases included three tasks designed to provoke a stress response in the participants, whereas the other three tasks were intended to reduce stress and support relaxation. Stress-inducing and stress-reducing tasks were alternated. An overview of the study protocol is given in Figure 4.1. The respective tasks are described in more detail in the following section.

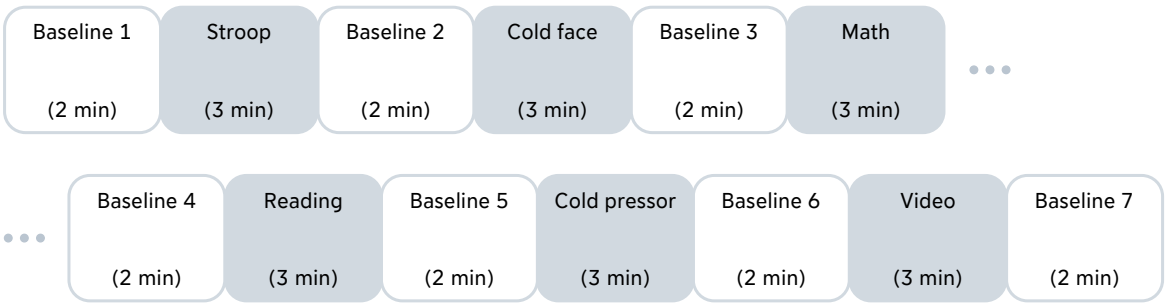

Figure 4.1: Study protocol consisting of six stress-inducing or -reducing tasks with baseline phases before the first task, after the last task, and between tasks.

Task 1: Stroop Test

The Stroop Test, which is a mental stress test and also referred to as the Stroop Color Word test, was first described by John R. Stroop. In the original test, the participant is asked to read 100 words out loud as fast as possible. The words presented are color words but are written in a font color that does not match the respective word, for example, the word ”red” is written in blue font. Due to this incongruence, it takes the brain longer to process the information and verbalize the correct word [Str35]. The mental overstimulation caused by cognitive conflict and the additional time pressure was found to trigger stress. Researchers observed increased concentrations of plasma epinephrine, urinary epinephrine, and plasma norepinephrine, all of which indicate increased SNS activity [Hos97; Tul89].

Accordingly, in the study conducted, an online version of the Stroop Test, where participants need to state the correct word via a button on the keyboard, is completed by the subjects with the aim of triggering increased sympathetic activity [Sto17; Sto10].

Task 2: Cold Face Test

When a cold stimulus is applied to the face, the PNS is activated, which is often referred to as the diving reflex and is usually provoked by immersion of the face in cold water [Lin09]. More precisely, cooling the eye and forehead region causes the excitation of the ophthalmic and maxillary branches of the trigeminal nerve. As a result, the vagus nerve, which is the central part of the PNS, is stimulated through the trigeminal-vagal reflex arc [Lem15]. In order to trigger the diving reflex and, thus, PNS activation in a more practical way, Khurana et al. proposed to cool the relevant facial areas by applying a cold stimulus instead of water

immersion. This approach is referred to as the Cold Face Test [Khu80]. Several studies have proven that the Cold face Test induces bradycardia, which is an indicator for heightened PNS activity [Ric22; Khu06; Hea90].

Correspondingly, the Cold Face Test is used within the conducted study as one of the relaxing phases as it is expected to increase PNS activity. A cooling mask (Dr. Winkler GmbH, Ainring-Mitterfelden, Germany) covering the majority of the facial area was applied for a duration of three minutes. The mask had a temperature of approximately 0 °C.

Task 3: Math Test

Mental stress, for example, provoked by demanding arithmetic tasks, is known to induce sympathetic activation as well as HPA axis activation [Rei04; Kir93]. Therefore, a mental arithmetic task is a part of the well-known Trier Social Stress Test described by Kirschbaum et al., which is a procedure that reliably induces stress in individuals [Kir93]. When performing this stress test, or mental arithmetic tasks in general, a subsequent increase of epinephrine and norepinephrine in the blood plasma was observed, which indicates heightened SNS activity [Tho12; Rei04].

Thus, a mental arithmetic task was included in the study as a stress-inducing phase. Within this phase, the study participants were asked to solve several mental arithmetic problems using an interactive computer program. Besides the arithmetic task, the program displayed several evaluative elements, such as a timeline, to additionally create time pressure. Also, the difficulty of the tasks was adjusted to the performance of the user, in order to make the tasks more challenging if necessary. These evaluative elements further increased the participant's stress level [Ric23].

Task 4: Reading

Motion artifacts are a common problem regarding the acquisition of cardiac parameters with wearable and contactless recording techniques, as these are typically used with the aim of allowing the participant's to behave fairly naturally and to ideally not restrict movement. Various types of motion artifacts can occur, for example, caused by walking, limb movements, or speaking [Her22; Keb20; Kum16].

In the case of the study conducted in this thesis, the participants' movement was partly restricted since data acquisition was performed in a sitting position, hence motion artifacts were mostly prevented. Consequently, only the robustness of the investigated PEP estimation

approaches against artifacts caused by speaking could be examined. For this purpose, a speaking phase was included in the study protocol in which participants were asked to read a text aloud. Besides, the speaking phase was also intended to have a relaxing effect on the participant.

Task 5: Cold Pressor Test:
The so-called Cold Pressor Test is a procedure widely used in medical settings to assess cardiovascular reactivity, as well as pain tolerance. During the Cold Pressor Test, a person's hand or foot is immersed in ice-cold water for a short period, typically two or three minutes. Researchers observed elevated blood pressure as a response to this procedure [Lov75]. In line with this, it was found that the Cold Pressor Test triggers the release of epinephrine and norepinephrine, which causes arteriolar vasoconstriction and thus elevates blood pressure. Based on the observed rise in epinephrine and norepinephrine concentration in the plasma, it can be inferred that the Cold Pressor Test leads to an increase in SNS activity [Vel97; War83].

Accordingly, a Cold Pressor Test was carried out with the participants of the study, which served as the third stress-inducing phase. The participants were instructed to immerse their right hand into approximately 0 °C cold water for the duration of three minutes or as long as possible. When the pain or discomfort got unbearable, the participant was allowed to remove their hand.

Task 6: Video
As the final relaxation phase of the study, the participants were shown a video of natural sceneries accompanied by calming music. Viewing soothing videos was reported to significantly decrease the concentration of sAA which indicates decreased ANS activity [Tak04]. Moreover, listening to relaxing music was found to decrease sAA levels as well, and thus to potentially have a stress-reducing effect [Lin15].

4.1.2 Measurements

As the objective of this work was to perform PEP measurement using different approaches, multiple kinds of data were recorded while the participants performed the previously outlined tasks.

Reference PEP Measurement ($\mathbf{PEP_{REF}}$)

To be able to evaluate the feasibility and the performance of the implemented PEP estimation techniques, reference signals were obtained. Following the gold standard PEP-measurement method, reference data consisting of ECG and ICG were recorded conventionally with electrodes attached to the skin and connected to the measurement device via cables. For this purpose, a BIOPAC device (BIOPAC Systems, Inc., CA 93117, USA) with an ECG100C and a NICO100C module for ECG and ICG recording, respectively, as well as the corresponding AcqKnowledge® software (BIOPAC Systems, Inc., CA 93117, USA) was utilized.

The ECG recording was performed according to Einthoven's Lead II configuration [Ein08], thus three electrodes were attached at the right clavicle, and at the right and left lower thorax [Bio21a; Bio19].

For the acquisition of the ICG data, eight electrodes are attached in pairs along the right and left mid-axillary lines, two each at the right and left side of the neck, and two each at the right and left side of the lower thorax [Bio21b; Deh19]. The ICG module of the BIOPAC device injects a small sinusoidal current of 400 µA through the thoracic region of the body. The module records the impedance magnitude (range 0–100 Ω), additionally the AcqKnowledge® software internally calculates the dZ/dt signal (range $\pm$ 2 $\Omega/\mathrm{s}/\mathrm{V}$).

Both the ECG and the ICG data are recorded with a sampling rate of 1000 Hz [Bio21a; Bio21b]. Figure 4.2 shows the electrode placement for ECG and ICG recordings.

PEP Measurement using wearable sensors ($\mathbf{PEP_W}$)

To realize PEP assessment without requiring wired connections, two wearable sensors (Portabiles NilsPod, Portabiles GmbH, Erlangen, Germany) were used. To capture the PEP start point, a portable ECG sensor is affixed to the participant's thorax with a chest strap approximately at the lower pectoral level. Hence, a 1-channel ECG was recorded according to Lead I of Einthoven's triangle [Ein08].

Additionally, the participants were equipped with a second sensor, which was attached approximately at the center of the sternum. In order to achieve minimal attenuation when recording the chest's micro-vibrations, the sensor was attached in direct skin contact using an adhesive foil. The sternum sensor, as well as the ECG sensor, recorded 6-d IMU data consisting of 3-d acceleration (range $\pm$ 16 g) and 3-d angular rate (range $\pm$ 2000 $^\circ/\mathrm{s}$). The thereby acquired ACC signals built the SCG data and were used to extract the PEP endpoint.

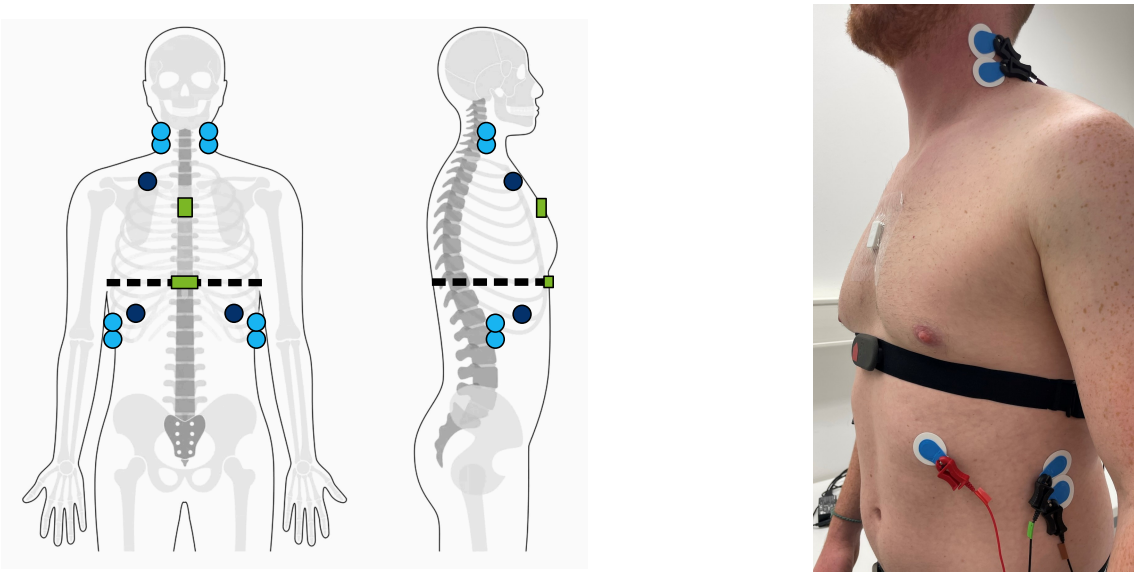

(a) **(b)**

Figure 4.2: Placement of ECG (dark blue) and ICG (light blue) electrodes required for reference PEP measurement, and wearable sensors (green) required for PEP estimation

Sensor data were logged onto each sensor's internal storage with a sampling rate of 256 Hz and transmitted to a computer for further processing. Also, both sensors were synchronized wirelessly, therefore subsequent synchronization is not necessary [Rot18]. The placement of these wearable sensors is shown in Figure 4.2.

PEP Measurement using radar and wearable ECG (PEP_{RAD})

For the radar-based PEP estimation approach, radar data was collected with two radar nodes developed by the subproject A04 of the EmpkinS collaborative research center [Emp23].

These radar nodes were installed in front (frontal) of and behind (dorsal) the participant, respectively, in order to compare the results of both positions. The frontal radar was pointed to the lower pectoral area of the participant, while it was ensured that it was pointed in between the two chest-worn sensors to avoid obstructing the path of the radar waves. The dorsal radar was targeted at the lower back. Since the back of the chair used for the study was made of fabric, the radar signal penetrated through it unhindered. Moreover, both radar sensors were aligned parallel to the body surface in order to best capture the signal reflected back from the body. A schematic illustration of the radar setup can be seen in Figure 4.3. The results of a preceding research work, which dealt with the ideal positioning of radars for heart rate

Figure 4.3: Positioning of the frontal and dorsal radar sensor nodes (orange)

monitoring, indicated that the best results might be achieved with the dorsal radar [Her22]. Accordingly, this was also expected in the study carried out here, but nevertheless, the frontal positioning was also included.

The in-phase (I) and quadrature (Q) components of the radar signal were recorded with a sampling rate of 1953 Hz. As the radar signal only contains information corresponding to the PEP endpoint, the wearable ECG data is utilized additionally to capture the PEP start point.

4.1.3 Data Cleaning and Preprocessing

Data Cleaning

The recorded dataset initially consisted of 22 participants with 32 minutes of recording each. The dataset can be thought of as three subsets corresponding to the three approaches for PEP extraction: the reference subset (ECG + ICG), the wearable sensor subset (SCG + ECG_W), and the radar subset (radar + ECG_W).

Regarding the reference data, no problems occurred during data acquisition, resulting in valid reference data from 22 persons. However, it was necessary to exclude the data of several participants from each of the two remaining subsets. Unfortunately, the wireless ECG sensor did not record any data for one participant, therefore this participant was excluded from the wearable sensor subset, as well as the radar subset. Additionally, a second participant needed to be excluded from the wearable and radar subsets because the sensor attached to the sternum lost connection during the data acquisition. The synchronization of all recorded data types was carried out using a dedicated synchronization signal transmitted to all recording devices, which will be discussed in more detail below. However, the transmission of this

synchronization signal to the radar device did not function properly for eight participants, therefore the synchronization of the respective radar data is impossible. Since variations of the PEP value in the range of milliseconds should be recorded, precise synchronization of the data is crucial. Consequently, the data of these 8 participants needed to be excluded from the radar subset.

Consequently, the wearable sensor subset contained the data of 20 persons, whereas the radar subset contained the data of only 12 persons. The reference subset included the data of all 22 participants. Although the demographic and anthropomorphic data hardly varied between the subsets, an overview of this information split up for each subset is given in Table 4.1.

Although the radar data was obtained during the study, it was decided that further evaluation of this data exceeded the scope of this work. Thus, it is not considered in the following parts of this thesis. However, it still remains part of the corresponding dataset in order to enable further analysis in the future.

Table 4.1: Demographic and anthropometric data of the participants of the main dataset (reference dataset) and two subsets (wearable sensor subset and radar subset); Mean $\pm$ SD

	#	f / m	Age [years]	Height [cm]	Weight [kg]
Reference subset (ECG + ICG)	22	11 / 11	24.9 $\pm$ 2.2	178.0 $\pm$ 9.2	73.2 $\pm$ 9.4
Wearable sensor subset (SCG + ECG_W)	20	10 / 10	24.6 $\pm$ 2.1	178.1 $\pm$ 9.3	73.3 $\pm$ 9.6
Radar subset (radar + ECG_W)	12	6 / 6	24.6 $\pm$ 2.5	176.8 $\pm$ 9.2	72.8 $\pm$ 11.3

Synchronization

For all implemented pep estimation methods, the start point and the end point of the PEP need to be extracted from separate signals, since the PEP start point and the PEP end point correspond to an electrical and a mechanical event, respectively. Additionally, the PEP is a relatively short cardiac interval of only approximately 100 ms [Hou05]. Accordingly, the PEP itself and its changes should ideally be measured accurately, at least to the millisecond. In

order to achieve such precise results, accurate synchronization of the used signals is crucial [Deh19].

Within the dataset acquired for this thesis, the ECG and ICG reference data are already recorded synchronously by the BIOPAC device [Bio22]. Similarly, the data acquired by the ECG_W sensor and by the IMU sensor attached to the sternum were also already synchronized wirelessly during the recording process [Rot18]. consequently, the global synchronization of the reference data, the wearable data, and the radar data still had to be realized.

This was accomplished by utilizing a custom-built synchronization board, which was developed within the EmpkinS project [Emp23]. All data recording devices were linked to the synchronization board via a wired connection. Obviously, in the case of the wearable sensors, such a cable connection was to be avoided to ensure that this approach nevertheless remained wireless. Therefore, an additional third sensor, which operated synchronously with the other two wearable sensors, was connected to the synchronization board. As this third sensor can just be stationary and does not need to be attached to the body, the wearable sensor data could also be included in the global synchronization, yet still remaining wireless. After the recording was started, the synchronization board transmitted a specific synchronization signal simultaneously to all connected devices. Each measurement device recorded this synchronization signal via a separate channel to allow for straightforward extraction and to prevent corruption of the actual data. Different shapes for the synchronization signal can be selected manually, depending on the use case. Here, a single peak was utilized. In a subsequent processing step, the *biopsykit* package [Ric21] is used to precisely align the time axes of all signals according to this synchronization peak. This procedure facilitated the precise temporal alignment of all acquired data.

Data Preprocessing

In addition to global synchronization of the acquired data, further preprocessing steps were required before the fiducial points needed for PEP estimation could be extracted. Firstly, filtering of the signals was performed in order to reduce noise and artifacts. For this purpose, suitable filters, as well as filter parameters, were selected for each type of signal. Secondly, since this work aimed for beat-to-beat PEP estimation, the reference and the wearable ECG data were segmented into single heartbeats. These preprocessing steps are outlined in more detail hereafter.

Both ECG signals, the reference ECG recorded with the BIOPAC, and the wirelessly recorded ECG_W, were cleaned using the *neurokit* python library [Mak21]. Since ECG signals are often corrupted by low-frequency baseline wander and high-frequency electromyographic noise, a bandpass filter is usually applied to remove or at least reduce such noise. Moreover, in most cases, powerline interference occurs, which should also be removed before further processing [Mir21]. The *neurokit* library cleans the ECG signal by applying a finite impulse response filter with a Hamming window in forward and backward direction [Mak21].

For ICG preprocessing, the literature proposes several options, including Savitzky-Golay, elliptic, and Butterworth filters, as well as Daubechies wavelets [Ben17]. For this thesis, filtering was performed with a 4th order Butterworth bandpass filter with 0.5 Hz and 25 Hz as low and high cutoff frequencies, respectively, which was applied forward and reverse [For19].

The initial step of the SCG preprocessing procedure implemented within this work, is the calibration of the IMU data that was recorded by both wearable sensors data. Therefore, a so-called Ferraris calibration is performed using the python library *imucal* [Küd22; Fer94]. The sensors' axes build a right-handed coordinate system and were defined as follows: the sensor's x-axis corresponds to the body's left-to-right axis, the sensor's y-axis corresponds to the body's craniocaudal axis, and the sensor's z-axis corresponds to the body's dorsoventral axis [Ahm19]. The axis configuration is depicted in Figure 4.4. Within most studies reported in the

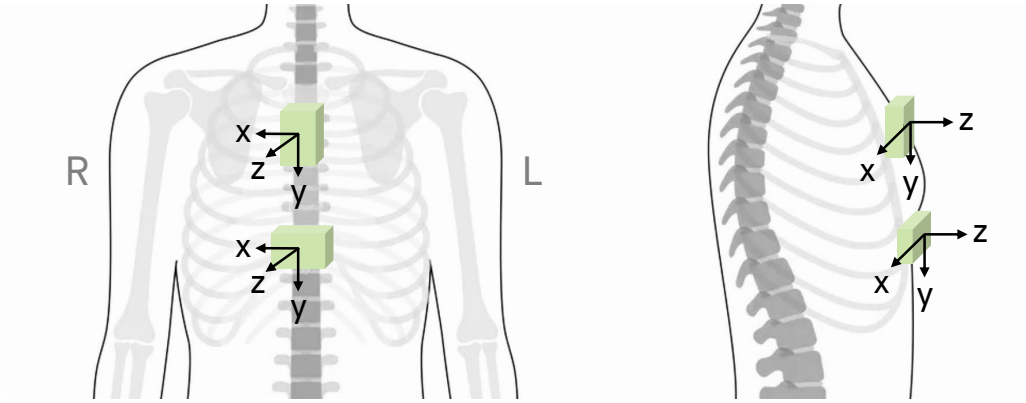

Figure 4.4: Axes configuration of the wearable sensors

literature, the chest's dorsoventral acceleration, which is equivalent to the ACC's z-component for the configuration employed in this work, is considered to be the SCG signal. However, for the AO extraction algorithm presented by Ahmaniemi et al., which was also implemented

within this thesis, all three ACC components of the IMU data were used [Ahm19]. Although the GYRO data acquired by the IMUs is not included in SCG-based cardiac assessment, it is thought to also contain insightful information about cardiac timings [Deh19; Sha19; Jaf17]. However, this aspect was not investigated within the scope of this thesis, since the relation of AO timing and the GYRO waveform was so far not explored extensively in the related literature [Deh20].

In order to facilitate fiducial point extraction from the SCG waveform, the according ACC signals are filtered to reduce noise and artifacts caused, for example, by body movement. The filtering is carried out with a forward-reverse application of a Butterworth bandpass filter with 5 Hz and 40 Hz low and high cutoff, which was proposed by Di Rienzo et al. [Di 17].

Prior to fiducial point extraction, all signals were segmented into single heartbeats as the goal of this thesis was to perform PEP assessment on a beat-to-beat level. The heartbeats were defined based on the ECG signal. Firstly, the R-peaks were detected using the *neurokit* library [Mak21], and RR-intervals to the respective preceding heartbeat were calculated. Then, the start of each heartbeat was set at a certain distance before the R-peak, which was defined as 35 % of the RR-interval with respect to the preceding heartbeat. The end of each heartbeat was defined as the start of the next one, therefore it corresponds to 65 % of the RR-interval with respect to the successive heartbeat after the current R-peak. Thus, it is ensured that the heartbeats directly follow each other. This procedure is similar to the heartbeat segmentation provided by the *neurokit* library. However, the approach implemented in *neurokit* introduced a fixed heartbeat duration by setting the heartbeat borders at 35 % of the mean RR-interval before the R-peak [Mak21]. This can produce overlapping heartbeats, as well as gaps between heartbeats. The data recorded for this thesis are suspected of having varying HR, which presumably results in highly overlapping heartbeats in parts of the signal. To avoid such overlaps, the heartbeat borders were set adaptively with regard to the current HR.

4.2 Fiducial Point Detection

As mentioned previously, to be able to extract the PEP, it is necessary to detect the fiducial points corresponding to PEP start and end in the respective signals. As the delineation and analysis of ECG signals is arguably the most commonly performed task in biomedical signal analysis, the according techniques and algorithms were extensively explored. Hence, a variety of signal processing packages are publicly available, such as the *neurokit* library. Thus, the

ECG fiducial point detection is based on the functionalities provided by this library. Contrarily, there are currently no algorithms realizing ICG and SCG waveform analysis that could be considered standardly applied or adequately researched. Consequently, some algorithms for the detection of the required fiducial points in these signals were implemented within this thesis. The algorithms were mainly based on certain selected approaches proposed in the literature, with some slight modifications made.

4.2.1 Detection of ECG Q-Peaks

According to the physiological definition, the PEP start point is equivalent to the onset of ventricular depolarization and thus to the onset of the Q-wave in the ECG signal [Wei77]. However, automatic detection of the Q-onset is a challenging task. The Q-wave is, in many cases, not sufficiently pronounced within the ECG signal to be able to reliably detect its onset [Ber04]. Particularly, when the ECG is recorded according to Einthoven's Lead II configuration, a distinct Q-wave might not be visible. This is due to the fact that the Q-wave corresponds to the depolarization of the interventricular septum, which propagates approximately perpendicular to the Lead II axis and is therefore hardly or not at all captured. In addition, the electrical axis of the heart varies between individuals, which further complicates the detection of the Q-onset. Accordingly, it is often reported in the literature that the PEP start was set at the R-onset or the R-peak minus a certain fixed threshold instead in order to sustain reliable detection across individuals [For18; Lie13; Ber04]. In line with this, within the scope of this thesis, the PEP start was defined to be the Q-peak, which is commonly considered to be equivalent to the R-onset.

For detection of the Q-peak, it is necessary to first detect the R-peaks within the ECG signal to subsequently find one Q-peak per heartbeat. As the R-peaks were already extracted for the heartbeat segmentation, it was unnecessary to implement this step here. Then, the remaining fiducial points, including the Q-peak, were detected with an ECG delineation algorithm provided by the *neurokit* library, which detects signal waves and peaks based on discrete wavelet transforms [Mak21; Mar04]. Using this approach, the Q-peaks were extracted from the reference ECG signal, as well as from the wirelessly recorded ECG_W signal.

4.2.2 Detection of ICG B- and C-Points

To determine the timing of the PEP endpoint, it is required to locate the point of AO within each heartbeat. This event corresponds to the so-called B-point within the ICG signal, as mentioned previously. The literature proposes several algorithms for B-point detection in the ICG derivative signal (dZ/dt), however, most of them are associated with three main approaches. Some locate the B-point directly within the dZ/dt signal, whereas others utilize the second (dZ^2/dt^2) or third derivative (dZ^3/dt^3) of the ICG signal. Arbol et al., who compared these three methods within their work, reported that their third derivative-based algorithm performed best for B-point detection [Árb17]. Thus, this method for B-point detection was selected and implemented for this thesis.

Since the B-point does not correspond to a peak or minimum of the ICG signal, its detection is not straightforward. The B-point is defined as the onset of the rapid upslope of the signal towards its maximum, which is referred to as the C-point. Thus, the B-point corresponds to a slope change [She90]. To be able to correctly locate the B-point within the ICG signal, usually a search window is defined. The end of this search window is set at the C-point, whereas the start of the window is chosen diversely in the literature, for example, at 300 ms or 150 ms before the C-point [Árb17], or at the R-peak [Lab70]. For the B-point detection algorithm presented here, the search window was defined as the 150 ms preceding the C-point.

In general, the C-point is easily detectable in most cases, since it corresponds to the global maximum of each heartbeat ICG signal [Árb17; She90]. However, for the data acquired within this work, the C-point was initially not correctly detected in some heartbeats of several participants, most likely due to disturbances in the signal leading to a mismatch of the global ICG maximum and the C-point within the respective heartbeat. Consequently, also the subsequent B-point detection was error-prone since it is reliant on correct C-point locations. From a physiological perspective, the C-point corresponds to the peak aortic blood flow following the AO, hence the C-point should definitively occur after the R-peak while still being relatively close to it [She90]. A correction procedure was implemented to avoid falsely detected C-points and thus facilitate correct B-point detection. Initially, the most prominent ICG signal peaks were detected. Then, for heartbeats with more than one possible C-point, the respective resulting R-C-distance for each of these C-candidates was compared with the

average R-C-distance of the three preceding heartbeats. Finally, the C-candidate providing the least deviation from this average R-C-distance was selected.

The subsequent B-point detection was straightforward. Following the technique proposed by Arbol et al., the third derivative dZ^3/dt^3 of the ICG signal was calculated within the search window for each heartbeat. The third derivative describes the intensity of the slope change in the ICG dZ/dt signal, therefore the maximum of the third derivative marks the most rapid slope change, which is equivalent to the B-point. The search window ensures that other randomly occurring sharp slope changes do not result in wrongly detected B-points [Árb17]. An example of the detected fiducial points and the corresponding PEP is depicted in Figure 4.5.

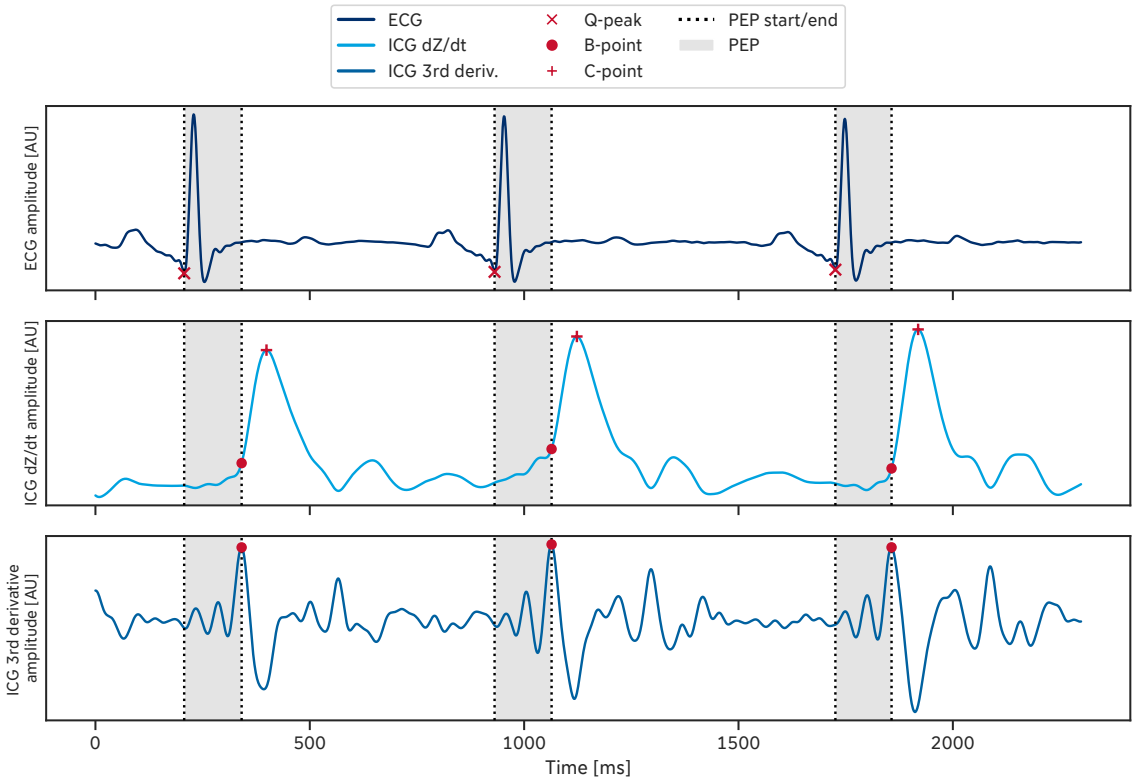

Figure 4.5: Extraction of the PEP reference from ECG and ICG signals with the B-point being set to the maximum of the ICG's 3rd derivative

4.2.3 Detection of Aortic Valve Opening in SCG

For PEP measurement based on wearable ECG and SCG data, the PEP start point is extracted from the ECG_W using the same approach as for the reference PEP, whereas the PEP endpoint, which corresponds to AO [Cro94], needs to be determined from the SCG waveform. The literature proposes several techniques to achieve this, two of which are implemented within this thesis. The first algorithm, which mostly follows the method proposed by Di Rienzo et al., detects the AO point in the dorsoventral component of the ACC signal [Di 17]. Contrarily, the second algorithm estimates the AO event from the complete triaxial ACC data [Ahm19]. In order to test different sensor placements, these algorithms were applied to the SCG data acquired by the sensor attached to the sternum, as well as to the one attached in the lower pectoral area, which simultaneously recorded the ECG_W.

In the dorsoventrally recorded SCG signal, the AO corresponds to a peak in the part of the signal associated with the systolic activity of the heart. Accordingly, for the first implemented AO detection algorithm, a search window of 200 ms starting at the R-peak was defined within each heartbeat as this part is considered to be the systolic portion of the signal. However, since the SCG waveform can vary considerably between individuals, the AO point is not necessarily equivalent to the global maximum within the systolic oscillations of the SCG signal. Consequently, some constraints needed to be introduced in order to select the correct peak and thus determine the correct AO timing. Instead of directly aiming to find the AO point, the point of isovolumetric contraction (IVC) is detected previously. Then the AO is selected afterward by taking the position of the IVC point into account. As the IVC corresponds to the first major minimum occurring consecutively to the R-peak and is clearly pronounced in most cases, it can generally be detected very easily. However, since wrongly detected IVC points might exist nevertheless, for instance, due to signal artifacts, an amplitude-based threshold t_{ICV} (see Equation 4.1) is introduced to discard minima occurring in smaller reflections.

$$y_{ICV} \leq \overline{y}_{window} - t_{IVC} \quad \text{with} \quad t_{IVC} = 0.5 * |y_{min} - \overline{y}_{window}| \tag{4.1}$$

The SCG signal amplitudes of the respective points are described by y, and signal baseline amplitude within the search window is described by $\overline{y}_{window}$. The threshold ensures that the chosen IVC is located sufficiently far beneath the signal baseline. Subsequently, for the AO, the first maximum following the IVC is selected. Similarly to the first threshold, a second amplitude-based threshold t_{AO} (see Equation 4.2) is defined in order to avoid wrongly

selecting the AO point due to small reflections following closely after the IVC.

$$y_{AO} \geq y_{ICV} + t_{AO} \quad \text{with} \quad t_{AO} = 0.7 * |y_{ICV} - \overline{y}_{window}| \tag{4.2}$$

The second threshold ensures that the AO point is located sufficiently high above the IVC. Introducing these thresholds reduces errors regarding the AO detection. Especially the second threshold t_{AO} is important since the signal peak associated with AO sometimes is still beneath the baseline of the signal, thus it should be avoided, for example, to rely on fixed amplitude thresholds [Di 17]. This algorithm is called the DV-ACC algorithm in the remainder of this thesis. Figure 4.6 exemplary depicts the AO and IVC points detected by using this algorithm, as well as the corresponding PEP.

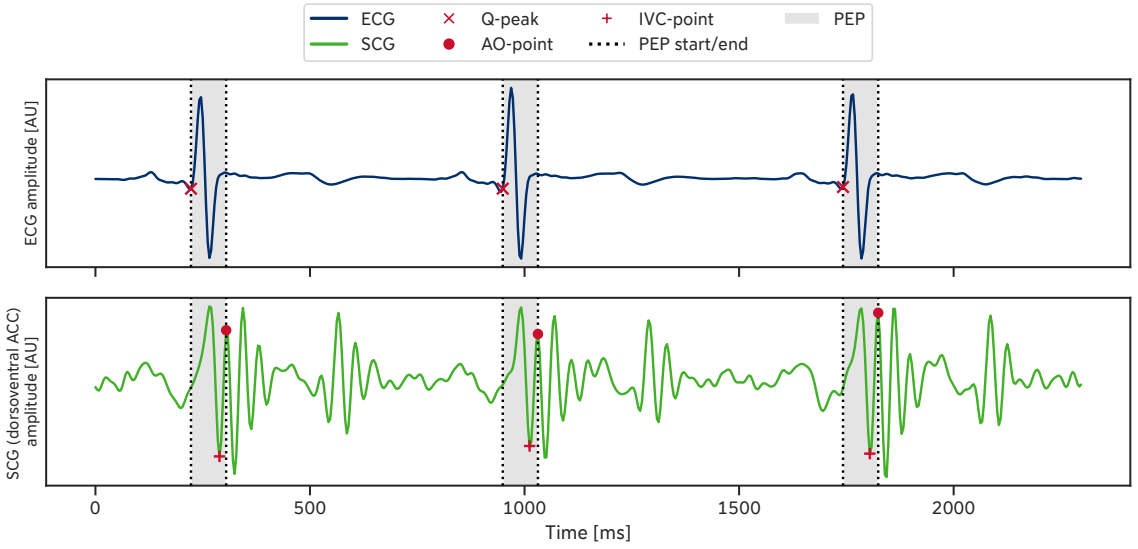

Figure 4.6: Extraction of the PEP from ECG_W and dorsoventral SCG signals

The second SCG-based AO detection algorithm explored within this thesis was proposed by Ahmaniemi et al. and used the signal envelope to estimate the timing of AO within each heartbeat. The same search window as in the first algorithm was applied, which consists of the 200 ms following the R-peak. As a first step, the L_2-norm of the three ACC signal components was calculated. Then, the resulting signal was highpass filtered with a cutoff frequency of 20 Hz. Afterward, the Hilbert envelope was constructed. This envelope was then squared and lowpass filtered again with a cutoff frequency of 20 Hz. For both filtering

steps, a 4th-order Butterworth filter was applied. Finally, the AO point was set according to the global maximum within the search interval of the envelope signal. This approach only approximates the timing of AO since it does not select its position according to the actual SCG waveform. However, this method is expected to be less affected by the variance of SCG waveforms across individuals [Ahm19]. This algorithm is referred to as the ENV-MAX algorithm in the following sections of this thesis. An overview of the processed signals and the detected fiducial points resulting from the application of this algorithm can be seen in Figure 4.7.

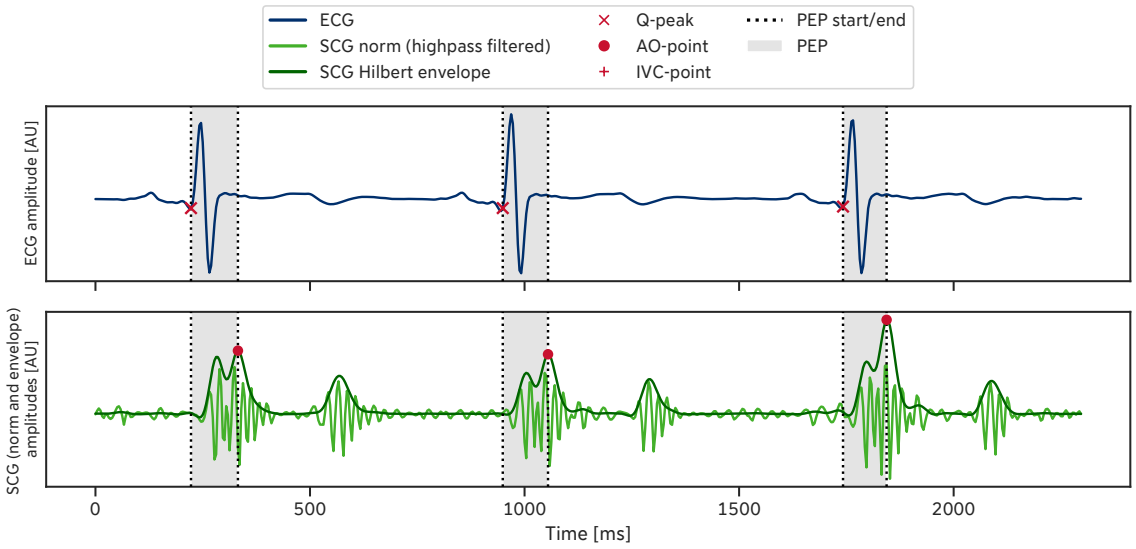

Figure 4.7: Extraction of the PEP from the ECG_W signal and the squared and lowpass filtered Hilbert envelope of the highpass filtered SCG signal norm (envelope is scaled up for better visibility)

4.3 Pre-Ejection Period Calculation

Obviously, determining the PEP value for each heartbeat is straightforward since it is given by the time difference between the start and endpoints. However, the PEP was calculated using start end endpoints extracted from different signals. In some heartbeats, the algorithms detecting the fiducial points were not able to locate any event considered correct with respect to the introduced constraints. For these cases, the algorithms marked the respective heartbeat

as invalid. Consequently, when either no valid start or no endpoint was present for a heartbeat, also the resulting PEP was marked as invalid. For the evaluation of the different PEP measurement approaches, only valid heartbeats were considered.

Firstly, the reference PEP values (PEP_{REF}) were determined from the conventional ECG and ICG recordings. Furthermore, PEP values were calculated using the ECG_W and the SCG signal obtained by the wearable sensors. These are referred to as PEP_W in the remaining chapters. For this wearable sensor-based PEP assessment method, separate PEP results were calculated for the SCG data acquired with the two differently placed IMU sensors, as well as for the two different AO extraction algorithms. As previously mentioned, the estimation of PEP using the radar data was unfortunately not possible within the scope of this thesis. An overview of the resulting types of PEP values and their respective description used in the following Results Chapter 5 is given in Table 4.2.

Table 4.2: Description of the different PEP extraction methods and their respective start and end points

	Description	**Start point**	**End point**
$\mathbf{PEP_{REF}}$	Reference PEP	ECG Q-peak	ICG B-point
$\mathbf{PEP^{W,\ sternum}_{DV\text{-}ACC}}$	PEP extracted from wearable sensor data (sternum sensor)	ECG_W Q-peak	SCG AO detected using dorsoventral ACC
$\mathbf{PEP^{W,\ lower\ pectoral}_{DV\text{-}ACC}}$	PEP extracted from wearable sensor data (lower pectoral sensor)	ECG_W Q-peak	SCG AO detected using dorsoventral ACC
$\mathbf{PEP^{W,\ sternum}_{ENV\text{-}MAX}}$	PEP extracted from wearable sensor data (sternum sensor)	ECG_W Q-peak	SCG AO detected using envelope max method
$\mathbf{PEP^{W,\ lower\ pectoral}_{ENV\text{-}MAX}}$	PEP extracted from wearable sensor data (lower pectoral sensor)	ECG_W Q-peak	SCG AO detected using envelope max method

Chapter 5

Results & Discussion

This section of the thesis presents the results and critically discusses them with respect to the related literature. All results were obtained based on the participants included in the wearable sensor subset combined with the respective reference data. Consequently, the used dataset was comprised of 20 participants.

5.1 Fiducial Point Detection Algorithms

One goal of this thesis was to implement several algorithms realizing the detection of the respective fiducial points in each type of signal. Within this work, the PEP values extracted from the dataset recorded with the BIOPAC using the implemented detection algorithms for Q-peak and B-point are considered to be the reference. As neither additional ground truth data was generated by manual labeling, nor a manual correction of the fiducial points detected by the algorithms was performed, it is not possible to actually evaluate the performance of the single algorithms. However, it is at least possible to examine how often each algorithm was able to produce results that were assumed to be valid or invalid.

5.1.1 Q-peak & B-point Detection in the Reference Dataset

Table 5.1 provides an overview of the mean absolute number and percentage of missed fiducial points per algorithm per participant for the algorithms used to extract the reference PEP (PEP_{REF}). The corresponding detailed results per participant can be found in Appendix A. The average total number of detected heartbeats per participant was approximately 2344

Table 5.1: Mean absolute number and percentage of missed fiducial points per participant for PEP_{REF} algorithms

	No Q		No B		No C	
# Heartbeats	**#**	**%**	**#**	**%**	**#**	**%**
2343.545	0.091	0.003	4.636	0.231	4.636	0.231

heartbeats, which corresponds to a mean HR of 73.25 beats per minute (bpm) for 32 minutes of recording. In only very few cases, in fact, in only for two heartbeats of a single participant, no Q-peak could be detected. This was to be expected, as the algorithm used for Q-peak detection provided by the *neurokit* library was reported to be able to detect the Q-peak in $> 99.9\,\%$ of the cases [Mar04].

Regarding the B-point, no valid event was found in approximately 5 heartbeats (0.231 %) per person. After further inspection, it was found that the vast majority of these missed B-points were caused by missing C-points, as the B-point detection algorithm did not attempt to determine the B-point if no valid C-point was present in the respective heartbeat. This even exceeded the B-detection performance achieved by Arbol et al. for their third derivative-based B-point detection algorithm, which was used as the foundation for the algorithm implemented here. They reported 3.6 % of missed B-points [Árb17]. Presumably, the number of missed B-points is decreased by the implemented C-point correction procedure.

5.1.2 Q-peak & AO-point Detection in the Wearable Sensor Dataset

For the data recorded by the wearable sensors, the average number of segmented heartbeats per person was approximately 2385. This deviation from the number of heartbeats detected from the conventionally recorded ECG signal can probably be explained by the fact that the ECG_W signal contains more motion artifacts than the signal acquired using electrodes, which could affect the heartbeat segmentation. The Q-peak detection algorithm failed for only very few heartbeats. The percentage of missed Q-peaks per person (0.002 %) is similar to the reference data.

Regarding the SCG data, no valid AO points could be detected on average in 0.164 % of the heartbeats using the DV-ACC algorithm and the data obtained with the sensor placed at the sternum. In contrast, for the second sensor attached in the lower pectoral area, the number of heartbeats, where no AO could be detected, was around seven times higher (1.105 %). A

possible explanation for this higher rate of missed AO points might be that the respective sensor, which simultaneously recorded ECG_W and IMU data, was attached to the person's chest by an elastic strap, whereas the sensor located at the sternum was attached with direct skin contact. Consequently, the mechanical coupling of the sternum sensor was probably better, resulting in less damping of the relevant micro-oscillations. Therefore, the SCG waveform might have been captured more precisely, enabling better AO detection. Furthermore, the sensor placement is presumably also a relevant factor. The SCG waveform is known to vary in shape when the sensor is not positioned at the sternum, which is the commonly used sensor placement [San20]. Moreover, the majority of waveform delineation techniques described in the literature are tailored to signal shapes being observed using this sensor configuration [Di 17; Ahm19; Ash18]. Accordingly, it is to be expected that the AO detection algorithm implemented here more robustly detects AO points in the signal recorded by the sternum sensor. Fittingly, Ashouri et al., who investigated the effects of different sensor placements for SCG-based PEP assessment, reported a higher RMSE for the PEP values obtained using an SCG sensor placed at the lower chest region compared to the conventional positioning [Ash18]. These findings indicate that the AO detection might be compromised when the sensor placement is altered. The described results can also be found in Table 5.2. Additionally, a more detailed version is included in Appendix A.

Table 5.2: Mean absolute number and percentage of missed fiducial points per participant for wearable sensor-based PEP (PEP_W) Q-peak and DV-ACC AO detection algorithms (S = sternum sensor; LP = lower pectoral sensor)

	No Q		No AO (S DV-ACC)		No AO (LP DV-ACC)	
# Heartbeats	**#**	**%**	**#**	**%**	**#**	**%**
2384.600	0.050	0.002	3.800	0.164	27.200	1.105

Besides performing the AO-point detection with the DV-ACC algorithm, the AO timings were also estimated using the ENV-MAX algorithm. However, as this algorithm simply assigns the AO point to the $argmax$ of the constructed envelope, heartbeats with missing AO-point can not occur. Hence, the average percentage of heartbeats where no fiducial point was detected is 0 %. That is why this algorithm is not listed in the corresponding tables.

To further investigate the implemented PEP measurement approaches, all heartbeats for which at least one of all used algorithms was not able to detect either the PEP start, the

end, or both, were discarded. Finally, a PEP result was obtained for 43573 heartbeats of 20 participants in total. Accordingly, for each participant, on average, 2178.65 heartbeats with a valid PEP value were obtained. In total, the average PEP detection ratio across participants was approximately 98.46 %, meaning that for 98.46 % of all heartbeats of one participant, it is possible to produce PEP results with all of the implemented algorithms.

Nevertheless, it should be noticed that, although in most heartbeats, all necessary fiducial points could be extracted and, thus, the PEP could be calculated, it still is not guaranteed that these points have the physiologically correct location. However, based on manual exemplary verification of the resulting fiducial points, it is assumed that the detected points mark the correct location of the respective event in the vast majority of the cases.

5.2 PEP during Stress-inducing and -reducing Tasks

One of the questions which should be answered by this thesis was whether the measured PEP actually changed during the stress-inducing and -reducing tasks performed throughout the study. Therefore, the reference PEP results were examined and the findings are described in this section of the thesis.

The reference PEP results, which were obtained from the conventional ECG and ICG recordings, do not show any major change between the different phases at first glance. This also becomes apparent in Figure 5.1 (a). The average mean PEP_{REF} across all participants was 138.30 ms. The mean standard deviation (SD) was $\pm$ 14.64 ms. The corresponding results per participant can be found in Appendix A.3. These values indicate, that the observed beat-to-beat PEP is highly variable. In order to investigate the reason for this observed wide PEP range, the PEP results of each individual study participant were examined. Figure 5.2 depicts the obtained PEP_{REF} results separately for all study participants. It becomes apparent that the range of measured PEP values is highly dependent on the individual. Correspondingly, also the SD of the mean PEP per person, which is $\pm$ 17.08 ms supports this finding. This highlights that the mean PEP varies considerably between individuals, which is in line with the literature [Kro17; Cac94b].

Furthermore, it is worth noticing that whether the PEP level changes according to the stress-inducing and -reducing tasks is also highly dependent on the individual. For example, for participants 4 and 6, it is clearly visible, that the average PEP during the Stroop and the Math task is lower than for the Cold Face and the Video task. This fits the expectation that

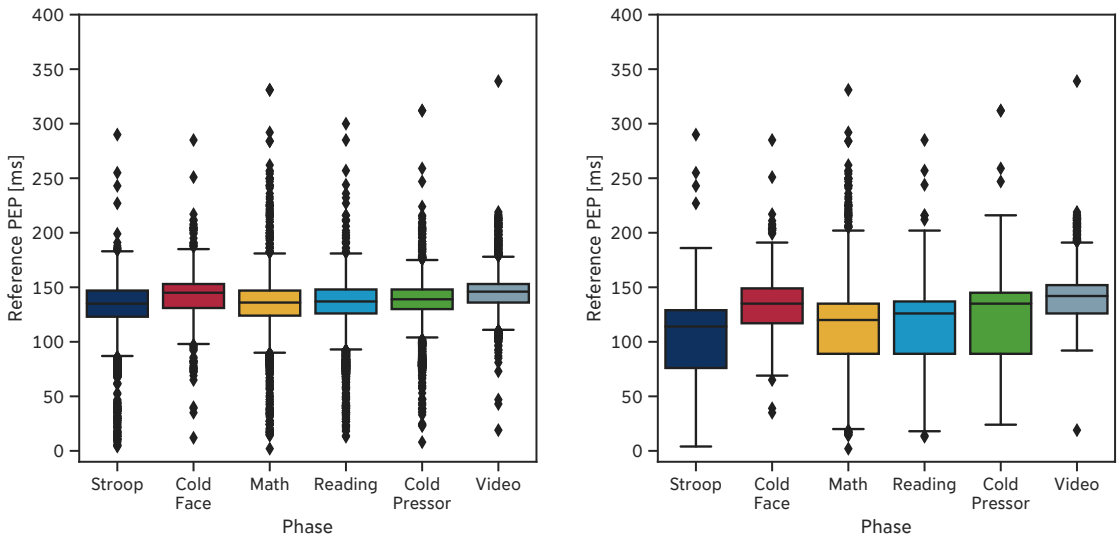

Figure 5.1: Boxplots of PEP_{REF} per phase for all participants (a) and responders (b)

tasks perceived as stressful induce a decrease in PEP compared to tasks that do not induce stress or even support relaxation. Correspondingly, the related literature also reports decreased PEP while participants performed certain tasks known to provoke stress and, thus, an SNS activity increase. For instance, Krohova et al. reported a decreased PEP induced by a mental arithmetic task [Kro17]. Also, Rahman et al. reported a decrease in PEP duration while study participants performed a Stroop Test [Rah18].

It is a well-established fact that individuals exhibit varying degrees of perceived stress in response to stressful situations, and, additionally, the individual physiological response to stressors also differs [Rus19; Oba17; Hel12]. It was, therefore, to be expected that the stress response to the different tasks indicated by the PEP change would differ between participants. As a sufficient variation in PEP was not present for all study participants, it was decided to split the dataset into a stress-responder and a non-responder group, to be able to investigate the results obtained from the responder group further. Since the Stroop was assumed to cause the highest SNS activation and hence the most decrease in PEP values, while the Video task was assumed to best support relaxation, these two tasks were picked to evaluate if a person should be assigned to either the responder or the non-responder group. For this purpose, the difference of the mean PEP during these study phases was calculated for each participant. The

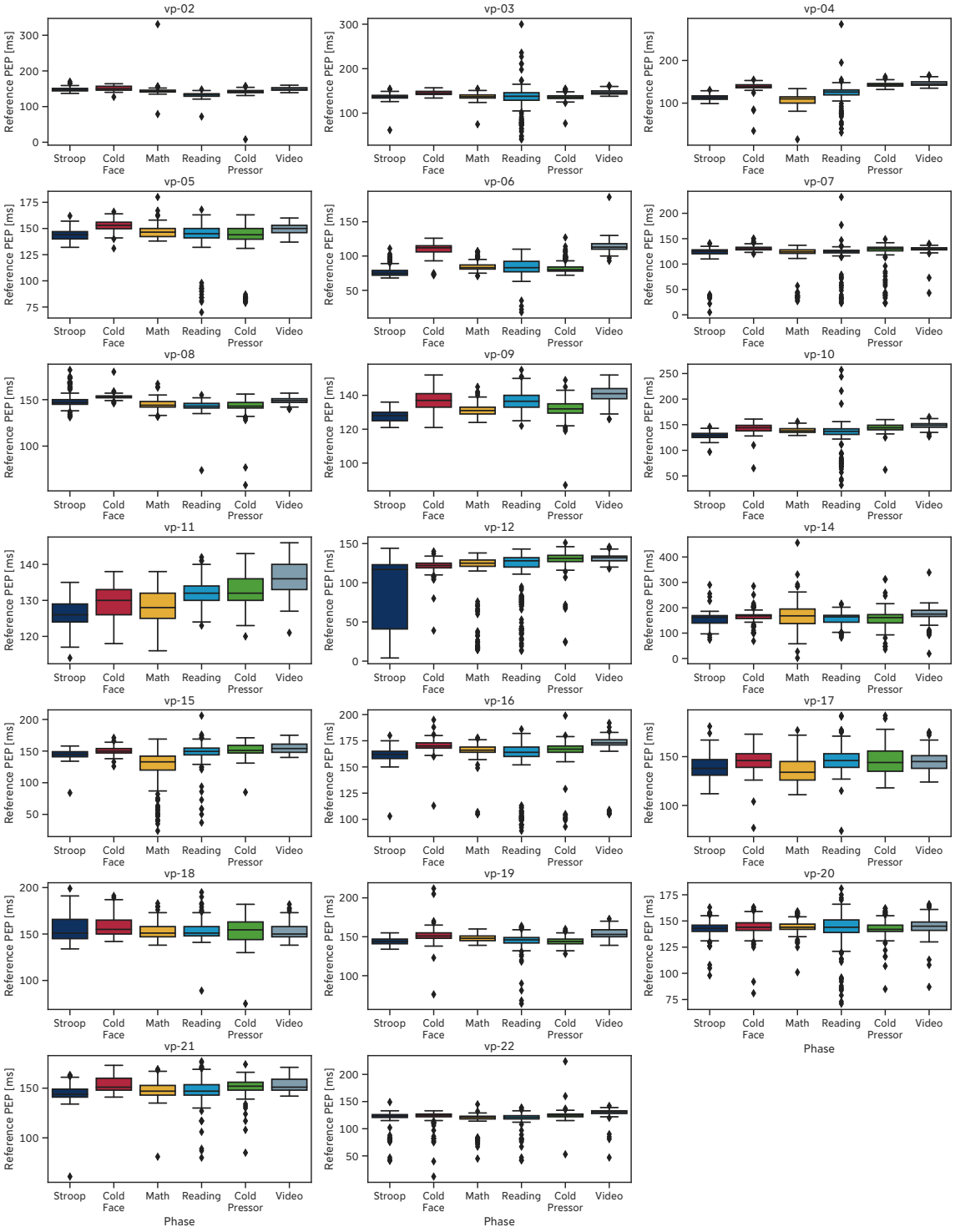

Figure 5.2: PEP_{REF} for all participants

corresponding results can be found in Table 5.3. Subsequently, the participants where a PEP difference of > 15 ms was observed, were assigned to the responder group. Consequently, the chosen participants are participants 4, 6, 10, 12, and 14, which are also highlighted in the table. The mean PEP values associated with the Stroop and Video phases for each participant assigned to the responder group can be found in Table 5.4, and a plot illustrating this information is given in Figure 5.3.

The mean PEP difference between the Stroop and the Video phase for the responder group was 30.65 ms. The difference of PEP values of the responders between these two phases is considerably higher than the mean SD (14.64 ms) of the entire observed PEP values across all participants and phases. This indicates, that the stress-inducing phases actually provoked a change in SNS activity and thus in PEP, at least for some of the participants.

Table 5.3: Table describing the difference of mean PEP_{REF} between Stroop and Video phase; responders are highlighted

Participant	**Diff. of Mean PEP [ms] (Stroop & Video)**
vp-02	1.273033
vp-03	10.114091
vp-04	**32.860753**
vp-05	5.594777
vp-06	**38.119165**
vp-07	8.340439
vp-08	-0.116690
vp-09	13.052690
vp-10	**19.508767**
vp-11	9.786782
vp-12	**40.461950**
vp-14	**22.300714**
vp-15	9.887272
vp-16	10.702683
vp-17	6.115909
vp-18	-2.596354
vp-19	9.799550
vp-20	2.429456
vp-21	7.914423
vp-22	11.279952

Table 5.4: Table describing the difference of mean PEP_{REF} between Stroop and Video phase for responders

Participant	Mean PEP [ms] Stroop Phase	Mean PEP [ms] Video Phase
vp-04	113.15	146.01
vp-06	76.14	114.26
vp-10	128.68	148.19
vp-12	91.05	131.51
vp-14	151.35	173.65
Summary	112.07	142.72

Conclusively, it can be stated that the study procedure applied in the study conducted for this thesis is actually, in general, suitable to induce a physiological stress response in individuals. As outlined in this section, a SNS activity increase could be observed in a group of participants indicated through a decreased average PEP value during the stress-inducing phase.

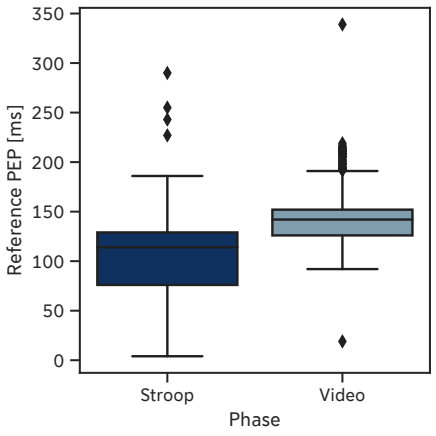

Figure 5.3: Boxplot of PEP_{REF} in Stroop and Video phase (responders)

5.3 Validity of the Wearable Sensor-based Approach

Moreover, this work aimed to evaluate whether it is possible to measure the PEP on a beat-to-beat level using wearable sensors. In this section, the validity of wearable sensor-based approaches is discussed in general. Exemplary, the $PEP^{W,\,sternum}_{DV\text{-}ACC}$ results obtained with the wearable ECG sensor in combination with the SCG data recorded by the sensor attached at the sternum are examined and compared to the reference data PEP_{REF}.

It should be noted that the feasibility of beat-to-beat PEP assessment based on wearable sensor data has only been examined in very few cases reported in the related literature [Deh19]. Instead, in most of the cases, the PEP results are median filtered over the complete duration of the respective study phase, or at least over one minute [Sha19; Ash18; Ahm19]. Thus, to be able to better compare the obtained results to the relevant literature, it was decided to also apply a median filter to the obtained results. In order to nevertheless preserve physiological PEP changes within a certain period of time, a smaller window (11 heartbeats) was chosen.

The agreement of the median filtered results for the PEP_{REF} method and the $PEP^{W,\,sternum}_{DV\text{-}ACC}$ approach is illustrated in the Bland-Altman plot in Figure 5.4. Accordingly, it can be stated that no sufficient agreement of both methods is achieved. The mean error of the $PEP^{W,\,sternum}_{DV\text{-}ACC}$ method is approximately 41.41 ms. Similar results are observed for the remaining wearable sensor-based approaches. These findings indicate that accurate PEP assessment using the techniques examined within this work on a beat-to-beat level and also for smaller median filtered time intervals is impossible.

However, this outcome can be explained as follows. The observed physiological range of the PEP_{REF} is 138.30 ± 14.64 ms. Since the mean measurement error of the $PEP^{W,\,sternum}_{DV\text{-}ACC}$ method is around 40 ms and thus considerably larger than the SD range of the PEP_{REF}, it becomes apparent that the wearable-sensor based method is not able to sufficiently capture the occurring variance in PEP. The reason for this is probably the limited time resolution of the utilized wearable sensors, as these are only recorded with a sampling frequency of 256 Hz. Consequently, the smallest time difference the sensors were able to capture was around 4 ms. Thus, in case the respective AO point of a heartbeat is missed even by only a few samples, this might already introduce an error in the range of > 10 ms for each of the two necessary fiducial points, which consequently would introduce even larger errors in the PEP results. As this issue is also present for the other implemented wearable sensor-based PEP measurement approaches, the corresponding results are not discussed in more detail here.

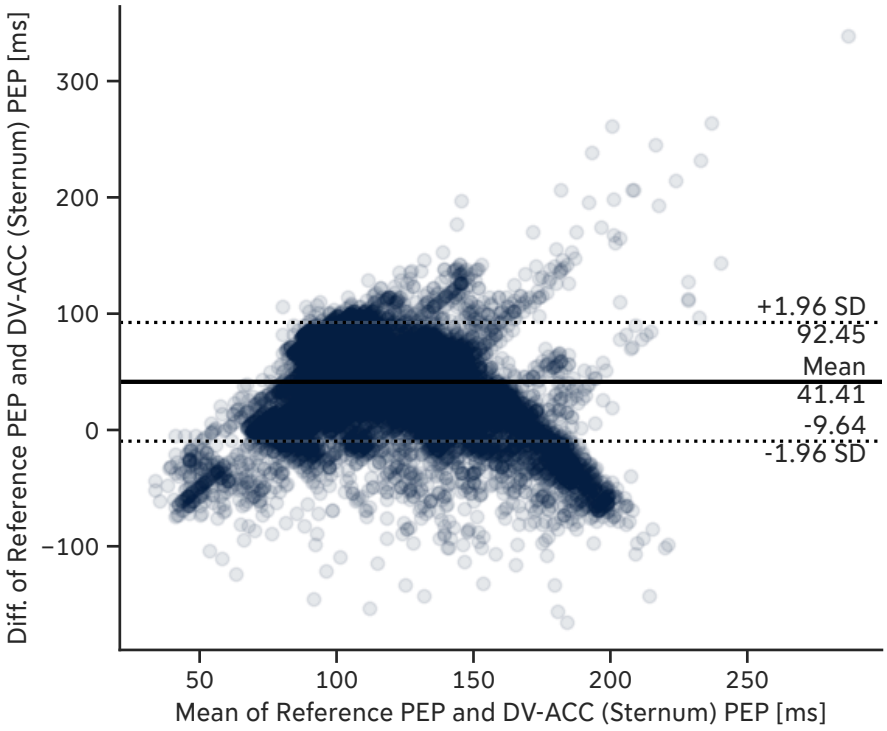

Figure 5.4: Bland-Altman Plot of PEP_{REF} and $PEP^{W,\,sternum}_{DV\text{-}ACC}$

However, regarding other wireless PEP assessment approaches described in the literature, the same issue arises, even though it might not always be apparent. For example, in the work of Dehkordi et al., beat-to-beat PEP estimation from SCG, data was presented. They reported a mean percentage error of 12.8 % compared to echocardiography-based ground truth. Although they did not report the range of occurring PEP values, it is presumably smaller than the one observed in the study conducted for this work since the data acquisition was performed with the participants in supine rest. Consequently, a measurement error of 12.8 % would most likely not allow accurate PEP measurement with respect to the observed physiological range of the PEP [Deh19]. Similarly, Shandhi et al., who examined SCG-based PEP estimation, reported a RMSE of 12.63 ms for their best-performing approach, while also not specifying the observed variation of PEP. Thus, the method developed by them probably is also not able to capture a physiologically relevant range accurately [Sha19]. Accordingly, the same shortcomings of the wearable sensor-based methods investigated within this thesis are in line with the related literature.

In order to overcome these issues, it is necessary to obtain the required signals with measurement equipment providing a higher time resolution in order to allow sufficiently accurate capturing of the physiologically relevant PEP range.

5.4 Detection of Stress States using Wearable Sensor-based PEP

Instead of aiming for beat-to-beat PEP assessment, another potential use case of the implemented wearable sensor-based PEP estimation techniques might be the detection of stress states in individuals. Within the group of stress responders, the performance of the wearable sensor-based PEP measurement methods was further investigated. Therefore, the obtained results of the Stroop phase and the Video phase were compared with respect to the different implemented approaches.

Figure 5.5 depicts the respective results for the $\text{PEP}_{\text{DV-ACC}}^{\text{W, sternum}}$, $\text{PEP}_{\text{DV-ACC}}^{\text{W, lower pectoral}}$, $\text{PEP}_{\text{ENV-MAX}}^{\text{W, sternum}}$, as well as the PEP_{REF} method. The corresponding effect sizes according to Cohen's d are given by $d = 1.17$ for PEP_{REF}, $d = 0.26$ for $\text{PEP}_{\text{DV-ACC}}^{\text{W, sternum}}$, $d = 0.98$ for $\text{PEP}_{\text{DV-ACC}}^{\text{W, lower pectoral}}$, and $d = 0.11$ for $\text{PEP}_{\text{ENV-MAX}}^{\text{W, sternum}}$. The associated results can be found in Appendix A.4, A.5, A.6, as well as in Table 5.4. The $\text{PEP}_{\text{ENV-MAX}}^{\text{W, lower pectoral}}$ method is not described here as its results were considerably worse. The described effect sizes highlight that the PEP estimation accuracy achieved by exclusively utilizing wearable sensors is sufficient to distinguish the phases associated with stress and relaxation, at least for some of the approaches. The wireless approach using the data acquired with the sensor with the lower pectoral positioning in combination with the $\text{PEP}_{\text{DV-ACC}}^{\text{W, sternum}}$ extraction technique was able to best capture the occurring PEP variation.

Unfortunately, none of the investigated wearable sensor-based PEP measurement approaches were sufficiently accurate to capture the PEP on a beat-to-beat level, which was primarily due to the limited precision of the utilized sensors. However, the results presented in this thesis indicate, that distinguishing between situations where an individual experiences stress and situations where the individual is rather relaxed is feasible using only wireless sensors.

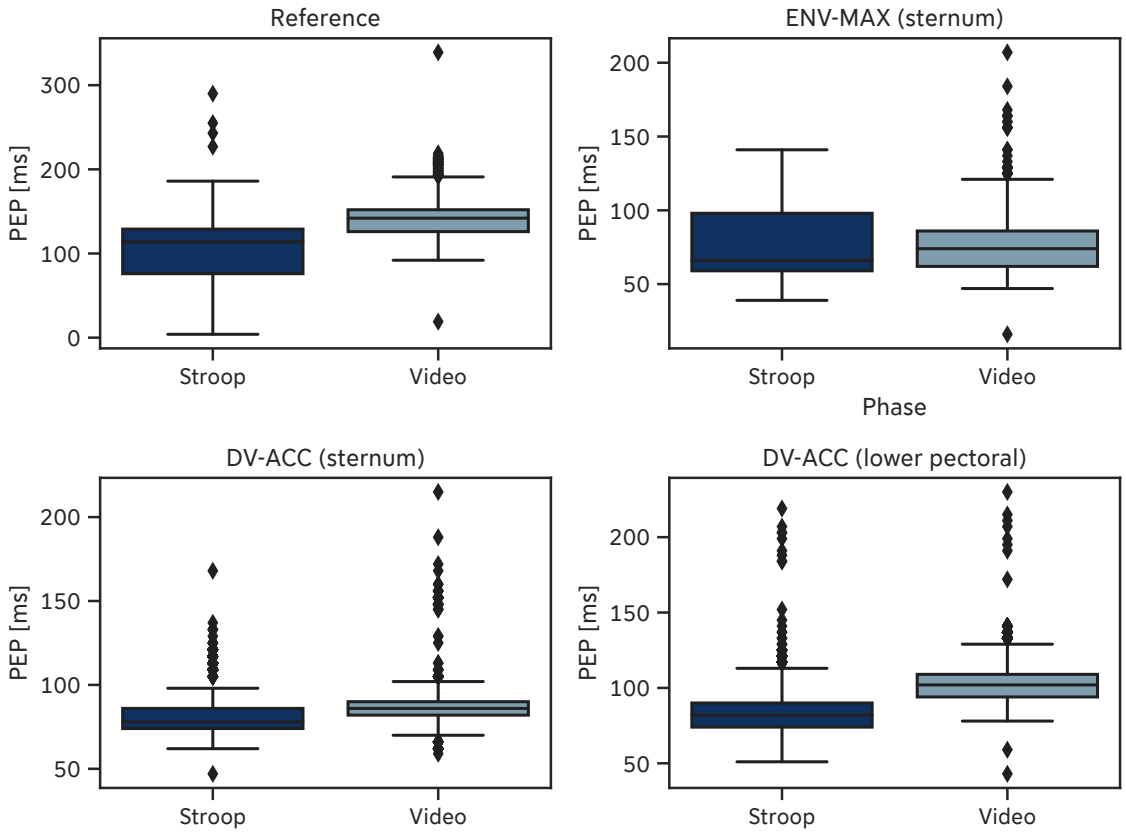

Figure 5.5: Boxplots of PEP in Stroop and Video phase for different PEP approaches (responders)

Chapter 6

Conclusion and Outlook

Although beat-to-beat PEP assessment using only wearable sensors could not be accomplished within this work, several helpful insights regarding wearable sensor-based PEP assessment could be gained.

In general, the implemented fiducial point extraction algorithms are presumed to identify the correct location of the respective events within the cardiac cycle. This assumption is based on two aspects. Firstly, the number of heartbeats where no fiducial point satisfying the respective conditions could be detected was very limited. Secondly, the detected fiducial points were manually checked by visual inspection and they were detected correctly for the vast majority of heartbeats. Nevertheless, comparing the extracted fiducial points to, for example, an expert-annotated ground truth would be beneficial in order to evaluate the performance of the implemented algorithms properly.

The main issue within this work was the limited time resolution of the utilized wearable sensors, which considerably impacted the PEP measurement accuracy. To overcome this, it is advisable to use sensors operating at a much higher sampling frequency than 1000 Hz. Thereby, it would be possible to capture the range of occurring PEP values more accurately.

However, use cases actually requiring a beat-to-beat PEP might be limited with respect to sympathetic and, thus, stress assessment, since situations during which individuals experience stress usually last for at least some minutes. Accordingly, the obtained results show that differentiation of situations perceived as stressful and not stressful is possible using the wearable sensor-based PEP measurement approaches. Hence, depending on the use case, it might be sufficient to obtain averaged PEP results for a certain period of time. Correspondingly,

the in this work developed, as well as further PEP assessment approaches are investigated within the EmpkinS D03 subproject. Within the project, a study collecting the same types of data as the study presented here is conducted. However, during this study, a more sophisticated stress test (Trier Social Stress Test [Kir93]) is performed, which probably provokes higher variation in PEP values. As also cortisol and sAA is measured during this study, the developed PEP estimation approaches can be evaluated with respect to well-established stress markers indicating the SNS activity.

Unfortunately, realizing PEP measurements using the interferometry radar data exceeded the scope of this thesis. However, this aspect should be investigated further in the future.

Conclusively, it can be stated that, even though accurate wearable sensor-based PEP measurement on a beat-to-beat level is not possible based on the obtained data, the developed PEP estimation algorithms enabled distinguishing stress-inducing and stress-reducing tasks.

Appendix A

Additional Tables

Table A.1: Missing fiducial points for PEP_W

Participant	# Heartbeats	No Q		No AO (S DV-ACC)		No AO (LP DV-ACC)	
		#	%	#	%	#	%
vp-02	1937	0	0.000	1	0.052	3	0.155
vp-03	2492	0	0.000	2	0.080	2	0.080
vp-04	2272	0	0.000	0	0.000	0	0.000
vp-05	1944	0	0.000	0	0.000	0	0.000
vp-06	3161	0	0.000	0	0.000	1	0.032
vp-07	2560	0	0.000	15	0.586	396	15.469
vp-08	2880	0	0.000	5	0.174	16	0.556
vp-09	2821	0	0.000	0	0.000	4	0.142
vp-10	2164	0	0.000	0	0.000	3	0.139
vp-11	2584	0	0.000	2	0.077	1	0.039
vp-12	2769	1	0.036	7	0.253	18	0.650
vp-14	2853	0	0.000	2	0.070	7	0.245
vp-15	1669	0	0.000	7	0.419	17	1.019
vp-16	2387	0	0.000	5	0.209	5	0.209
vp-17	2039	0	0.000	9	0.441	40	1.962
vp-18	2157	0	0.000	1	0.046	15	0.695
vp-19	2323	0	0.000	8	0.344	6	0.258
vp-20	2134	0	0.000	2	0.094	6	0.281
vp-21	2183	0	0.000	6	0.275	3	0.137
vp-22	2363	0	0.000	4	0.169	1	0.042

Table A.2: Missing fiducial points for PEP_{REF}

Participant	# Heartbeats	No Q		No B		No C	
		#	%	#	%	#	%
vp-01	2517	0	0.000	5	0.199	5	0.199
vp-02	1944	0	0.000	13	0.669	13	0.669
vp-03	2492	0	0.000	0	0.000	0	0.000
vp-04	2272	0	0.000	1	0.044	1	0.044
vp-05	1949	0	0.000	5	0.257	5	0.257
vp-06	3165	0	0.000	0	0.000	0	0.000
vp-07	2557	0	0.000	2	0.078	2	0.078
vp-08	2882	0	0.000	1	0.035	1	0.035
vp-09	2821	0	0.000	1	0.035	1	0.035
vp-10	2163	0	0.000	1	0.046	1	0.046
vp-11	2577	0	0.000	0	0.000	0	0.000
vp-12	2770	2	0.072	1	0.036	1	0.036
vp-13	1331	0	0.000	1	0.075	1	0.075
vp-14	2854	0	0.000	10	0.350	10	0.350
vp-15	1704	0	0.000	28	1.643	28	1.643
vp-16	2393	0	0.000	2	0.084	2	0.084
vp-17	2007	0	0.000	26	1.295	26	1.295
vp-18	2156	0	0.000	3	0.139	3	0.139
vp-19	2323	0	0.000	0	0.000	0	0.000
vp-20	2134	0	0.000	0	0.000	0	0.000
vp-21	2184	0	0.000	2	0.092	2	0.092
vp-22	2363	0	0.000	0	0.000	0	0.000

Table A.3: PEP_{REF} results; Mean and SD

Participant	Mean [ms]	± SD [ms]
vp-02	144.148768	11.222184
vp-03	139.157380	14.385585
vp-04	126.775952	19.457067
vp-05	145.456157	12.798078
vp-06	89.405742	15.808425
vp-07	123.534596	19.431377
vp-08	146.911234	6.944942
vp-09	134.072973	6.306040
vp-10	138.532982	14.858280
vp-11	130.924925	5.204640
vp-12	116.050951	30.180977
vp-14	161.004798	34.561162
vp-15	144.991860	20.157209
vp-16	164.796651	14.514026
vp-17	143.000000	13.264553
vp-18	154.525394	11.083571
vp-19	147.819739	8.480333
vp-20	143.500439	10.566251
vp-21	149.755383	9.884354
vp-22	121.730435	13.645172
Summary	138.304818 ± 17.08	14.637711

Table A.4: $PEP^{W,\,sternum}_{DV\text{-}ACC}$ results (responder)

Participant	Mean PEP [ms] Stroop Phase	Mean PEP [ms] Video Phase
vp-04	71.943396	78.257310
vp-06	74.754342	88.574766
vp-10	85.547511	90.380682
vp-12	76.199248	83.367965
vp-14	112.691176	97.092105
Summary	84.227135	87.534566

Table A.5: $PEP^{W,\text{ lower pectoral}}_{\text{DV-ACC}}$ results (responder)

Participant	Mean PEP [ms] Stroop Phase	Mean PEP [ms] Video Phase
vp-04	84.924528	102.649123
vp-06	70.287841	102.830986
vp-10	81.203620	97.215909
vp-12	90.293233	95.100000
vp-14	120.213235	134.890351
Summary	89.384492	106.537274

Table A.6: $PEP^{W,\text{ sternum}}_{\text{ENV-MAX}}$ results (responder)

Participant	Mean PEP [ms] Stroop Phase	Mean PEP [ms] Video Phase
vp-04	58.660377	64.923977
vp-06	58.640199	74.163551
vp-10	92.045249	79.869318
vp-12	64.398496	65.311688
vp-14	112.518382	113.894737
Summary	77.252541	79.632654

Appendix B

Acronyms

SNS sympathetic nervous system

PNS parasympathetic nervous system

ANS autonomic nervous system

HPA hypothalamic-pituitary-adrenal

sAA salivary α-amylase

AA α-amylase

ECG electrocardiogram

ECG_W wearable ECG

ICG impedance cardiography

PCG phonocardiogram

SCG seismocardiogram

BCG ballistocardiogram

IMU inertial measurement unit

FCG forcecardiogram

M-mode motion mode

ACC accelerometer

GYRO gyroscope

PEP pre-ejection period

$\mathbf{PEP_{REF}}$ reference PEP

$\mathbf{PEP_{W}}$ wearable sensor-based PEP

$\mathbf{PEP_{RAD}}$ radar-based PEP

$\mathbf{PEP^{W,\ sternum}_{DV\text{-}ACC}}$ wearable sensor-based PEP (sternum sensor, DV-ACC algorithm)

$\mathbf{PEP^{W,\ lower\ pectoral}_{DV\text{-}ACC}}$ wearable sensor-based PEP (lower pectoral sensor, DV-ACC algorithm)

$\mathbf{PEP^{W,\ sternum}_{ENV\text{-}MAX}}$ wearable sensor-based PEP (sternum sensor, ENV-MAX algorithm)

$\mathbf{PEP^{W,\ lower\ pectoral}_{ENV\text{-}MAX}}$ wearable sensor-based PEP (lower pectoral sensor, ENV-MAX algorithm)

LVET left ventricular ejection time

$\mathbf{QS_2}$ total electromechanical systole

IVC isovolumetric contraction

HR heart rate

HRV heart rate variability

AO aortic valve opening

MC mitral valve closure

AV node atrioventricular node

bpm beats per minute

RF radio frequency

IR infrared

LSTM long short-term memory

RMSE root mean square error

SD standard deviation

List of Figures

List of Tables

Bibliography

[Adi14] Fadel Adib, Zach Kabelac, Dina Katabi, and Robert C Miller. "3D Tracking via Body Radio Reflections". In: *Proceedings of the 11th USENIX Symposium on Networked Systems Design and Implementation (NSDI '14)*. USENIX Symposium on Networked Systems Design and Implementation (NSDI '14). Seattle, WA, USA, 2014. URL: https://www.usenix.org/conference/nsdi14/technical-sessions/presentation/adib (visited on 01/24/2023).

[Ahm19] Teemu Ahmaniemi, Satu Rajala, and Harri Lindholm. "Estimation of Beat-to-Beat Interval and Systolic Time Intervals Using Phono- and Seismocardiograms". In: *2019 41st Annual International Conference of the IEEE Engineering in Medicine and Biology Society (EMBC)*. 2019 41st Annual International Conference of the IEEE Engineering in Medicine and Biology Society (EMBC). ISSN: 1558-4615. July 2019, pp. 5650–5656. DOI: 10.1109/EMBC.2019.8856931.

[All14] Andrew P. Allen, Paul J. Kennedy, John F. Cryan, Timothy G. Dinan, and Gerard Clarke. "Biological and psychological markers of stress in humans: Focus on the Trier Social Stress Test". In: *Neuroscience & Biobehavioral Reviews* 38 (Jan. 2014), pp. 94–124. ISSN: 01497634. DOI: 10.1016/j.neubiorev.2013.11.005. URL: https://linkinghub.elsevier.com/retrieve/pii/S0149763413002728 (visited on 04/29/2022).

[APA19] APA. "Stress in America™ 2019". In: *American Psychological Association* (2019). URL: https://www.apa.org/news/press/releases/stress/2019/stress-america-2019.pdf.

[Árb17] Javier Rodríguez Árbol, Pandelis Perakakis, Alba Garrido, José Luis Mata, M. Carmen Fernández-Santaella, and Jaime Vila. "Mathematical detection of aortic valve opening (B point) in impedance cardiography: A comparison of three popular

algorithms: Mathematical detection of aortic valve opening". In: *Psychophysiology* 54.3 (Mar. 2017), pp. 350–357. ISSN: 00485772. DOI: 10.1111/psyp.12799. URL: https://onlinelibrary.wiley.com/doi/10.1111/psyp.12799 (visited on 11/15/2022).

[Ash16] Hazar Ashouri, Lara Orlandic, and Omer T. Inan. "Unobtrusive Estimation of Cardiac Contractility and Stroke Volume Changes Using Ballistocardiogram Measurements on a High Bandwidth Force Plate". In: *Sensors* 16.6 (June 2016), p. 787. ISSN: 1424-8220. DOI: 10.3390/s16060787. URL: https://www.mdpi.com/1424-8220/16/6/787 (visited on 01/27/2023).

[Ash18] Hazar Ashouri, Sinan Hersek, and Omer T. Inan. "Universal Pre-Ejection Period Estimation Using Seismocardiography: Quantifying the Effects of Sensor Placement and Regression Algorithms". In: *IEEE Sensors Journal* 18.4 (2018). Publisher: IEEE, pp. 1665–1674. ISSN: 1530437X. DOI: 10.1109/JSEN.2017.2787628.

[Atk09] Anthony Atkielski. *Schematic diagram of normal sinus rhythm for a human heart as seen on ECG*. Sept. 23, 2009. URL: https://commons.wikimedia.org/wiki/File:SinusRhythmLabels.png (visited on 03/27/2023).

[Bae64] Roman M. Baevsky, A. D. Egorov, and L. A. Kazarian. "The Method of Seismocardiography". In: *Kardiologiia* 18 (1964), pp. 87–89.

[Bai12] Jing Bai, Girum Sileshi, Glenn Nordehn, Stanley Burns, and Lorentz Wittmers. "Development of laser-based heart sound detection system". In: 2012 (Jan. 12, 2012). DOI: 10.4236/jbise.2012.51005. URL: http://www.scirp.org/journal/PaperInformation.aspx?PaperID=16935 (visited on 03/23/2023).

[Ben17] Ihsèn Ben Salah and Kaïs Ouni. "Denoising of the impedance cardiographie signal (ICG) for a best detection of the characteristic points". In: *2017 2nd International Conference on Bio-engineering for Smart Technologies (BioSMART)*. 2017 2nd International Conference on Bio-engineering for Smart Technologies (BioSMART). Aug. 2017, pp. 1–4. DOI: 10.1109/BIOSMART.2017.8095347.

[Ber04] Gary G. Berntson, David L. Lozano, Yun-Ju Chen, and John T. Cacioppo. "Where to Q in PEP". In: *Psychophysiology* 41.2 (Mar. 2004), pp. 333–337. ISSN: 0048-5772, 1469-8986. DOI: 10.1111/j.1469-8986.2004.00156.x. URL: https:

//onlinelibrary.wiley.com/doi/10.1111/j.1469-8986.2004.00156.x (visited on 11/15/2022).

[Ber94] Gary G. Berntson, John T. Cacioppo, Philip F. Binkley, Bert N. Uchino, Karen S. Quigley, and Annette Fieldstone. "Autonomic cardiac control. III. Psychological stress and cardiac response in autonomic space as revealed by pharmacological blockades". In: *Psychophysiology* 31.6 (Nov. 1994), pp. 599–608. ISSN: 0048-5772, 1469-8986. DOI: 10.1111/j.1469-8986.1994.tb02352.x. URL: https://onlinelibrary.wiley.com/doi/10.1111/j.1469-8986.1994.tb02352.x (visited on 08/25/2022).

[Bic17] A. Ozan Bicen, Nil Z. Gurel, Alexis Dorier, and Omer T. Inan. "Improved Pre-Ejection Period Estimation From Ballistocardiogram and Electrocardiogram Signals by Fusing Multiple Timing Interval Features". In: *IEEE Sensors Journal* 17.13 (July 1, 2017). Publisher: IEEE, pp. 4172–4180. ISSN: 1530-437X. DOI: 10.1109/JSEN.2017.2707061. URL: http://ieeexplore.ieee.org/document/7932412/.

[Bio19] Inc. Biopac Systems. *Application Note BIOPAC ECG*. 2019. URL: https://www.biopac.com/wp-content/uploads/app109.pdf.

[Bio21a] Inc. Biopac Systems. *BIOPAC-ECG100C Product Sheet*. 2021. URL: https://www.biopac.com/wp-content/uploads/EGG100C.pdf.

[Bio21b] Inc. Biopac Systems. *BIOPAC-NICO100C Product Sheet*. 2021. URL: https://www.biopac.com/wp-content/uploads/NICO100C.pdf.

[Bio22] Inc. Biopac Systems. *AcqKnowledge 5 - Software Guide*. 2022. URL: https://www.biopac.com/wp-content/uploads/AcqKnowledge-5-Software-Guide.pdf.

[Bot21] Angela Botros, Nathan Gyger, Narayan Schütz, Michael Single, Tobias Nef, and Stephan M. Gerber. "Contactless Gait Assessment in Home-like Environments". In: *Sensors* 21.18 (Jan. 2021), p. 6205. ISSN: 1424-8220. DOI: 10.3390/s21186205. URL: https://www.mdpi.com/1424-8220/21/18/6205 (visited on 01/24/2023).

[Bou90] H. Boudoulas. "Systolic time intervals". In: *European Heart Journal* 11 (suppl I Jan. 2, 1990), pp. 93–104. ISSN: 0195-668X, 1522-9645. DOI: 10.1093/eurheartj/11.suppl_I.93. URL: https://academic.oup.com/eurheartj/article-lookup/doi/10.1093/eurheartj/11.suppl_I.93 (visited on 03/27/2023).

[Bri14] Ryan C. Brindle, Annie T. Ginty, Anna C. Phillips, and Douglas Carroll. "A tale of two mechanisms: A meta-analytic approach toward understanding the autonomic basis of cardiovascular reactivity to acute psychological stress". In: *Psychophysiology* 51.10 (2014), pp. 964–976. ISSN: 1469-8986. DOI: 10.1111/psyp.12248. URL: https://onlinelibrary.wiley.com/doi/abs/10.1111/psyp.12248 (visited on 08/15/2022).

[Bur13] J. Burlingame, P. Ohana, M. Aaronoff, and T. Seto. "Noninvasive cardiac monitoring in pregnancy: impedance cardiography versus echocardiography". In: *Journal of Perinatology* 33.9 (Sept. 2013), pp. 675–680. ISSN: 1476-5543. DOI: 10.1038/jp.2013.35. URL: https://www.nature.com/articles/jp201335 (visited on 03/29/2023).

[Bux17] Dilpreet Buxi, Jean-Michel Redouté, and Mehmet Rasit Yuce. "Systolic time interval estimation at the sternum using continuous wave radar with body-contact antennas". In: *2017 IEEE 14th International Conference on Wearable and Implantable Body Sensor Networks (BSN)*. 2017 IEEE 14th International Conference on Wearable and Implantable Body Sensor Networks (BSN). ISSN: 2376-8894. May 2017, pp. 87–90. DOI: 10.1109/BSN.2017.7936014.

[Cac94a] John T. Cacioppo, Gary G. Berntson, Philip F. Binkley, Karen S. Quigley, Bert N. Uchino, and Annette Fieldstone. "Autonomic cardiac control. II. Noninvasive indices and basal response as revealed by autonomic blockades". In: *Psychophysiology* 31.6 (Nov. 1994), pp. 586–598. ISSN: 0048-5772, 1469-8986. DOI: 10.1111/j.1469-8986.1994.tb02351.x. URL: https://onlinelibrary.wiley.com/doi/10.1111/j.1469-8986.1994.tb02351.x (visited on 08/25/2022).

[Cac94b] John T. Cacioppo, Bert N. Uchino, and Gary G. Berntson. "Individual differences in the autonomic origins of heart rate reactivity: The psychometrics of respiratory sinus arrhythmia and preejection period". In: *Psychophysiology* 31.4 (July 1994), pp. 412–419. ISSN: 0048-5772, 1469-8986. DOI: 10.1111/j.1469-8986.1994.

tb02449.x. URL: https://onlinelibrary.wiley.com/doi/10.1111/j.1469-8986.1994.tb02449.x (visited on 08/25/2022).

[Can53] Walter B Cannon. "Bodily Changes in Pain, Hunger, Fear and Rage; An Account of Recent Researches into the Function of Emotional Excitement." In: *Science* 42.1089 (1953), pp. 696–700. ISSN: 0036-8075, 1095-9203. DOI: 10.1126/science.42.1089.696.b. URL: https://www.science.org/doi/10.1126/science.42.1089.696.b (visited on 01/21/2023).

[Cen22] Jessica Centracchio, Emilio Andreozzi, Daniele Esposito, Gaetano Dario Gargiulo, and Paolo Bifulco. "Detection of Aortic Valve Opening and Estimation of Pre-Ejection Period in Forcecardiography Recordings". In: *Bioengineering* 9.3 (Mar. 2022), p. 89. ISSN: 2306-5354. DOI: 10.3390/bioengineering9030089. URL: https://www.mdpi.com/2306-5354/9/3/89 (visited on 01/27/2023).

[Cro94] Richard S. Crow, Peter Hannan, David Jacobs, Lowell Hedquist, and David M. Salerno. "Relationship between Seismocardiogram and Echocardiogram for Events in the Cardiac Cycle". In: *American Journal of Noninvasive Cardiology* 8 (1994), pp. 39–46. ISSN: 0258-4425, 2504-2378. DOI: 10.1159/000470156. URL: https://www.karger.com/Article/FullText/470156 (visited on 01/27/2023).

[Deh19] Parastoo Dehkordi, Farzad Khosrow-Khavar, Marco Di Rienzo, Omer T. Inan, Samuel E. Schmidt, Andrew P. Blaber, Kasper Sørensen, Johannes J. Struijk, Vahid Zakeri, Prospero Lombardi, Md. Mobashir H. Shandhi, Mojtaba Borairi, John M. Zanetti, and Kouhyar Tavakolian. "Comparison of Different Methods for Estimating Cardiac Timings: A Comprehensive Multimodal Echocardiography Investigation". In: *Frontiers in Physiology* 10 (Aug. 22, 2019), p. 1057. ISSN: 1664-042X. DOI: 10.3389/fphys.2019.01057. URL: https://www.frontiersin.org/article/10.3389/fphys.2019.01057/full (visited on 05/13/2022).

[Deh20] Parastoo Dehkordi, Kouhyar Tavakolian, Mojtaba Jafari Tadi, Vahid Zakeri, and Farzad Khosrow-khavar. "Investigating the estimation of cardiac time intervals using gyrocardiography". In: *Physiological Measurement* 41.5 (June 10, 2020), p. 055004. ISSN: 1361-6579. DOI: 10.1088/1361-6579/ab87b2. URL: https://iopscience.iop.org/article/10.1088/1361-6579/ab87b2 (visited on 03/21/2023).

[Di 17] Marco Di Rienzo, Emanuele Vaini, and Prospero Lombardi. “An algorithm for the beat-to-beat assessment of cardiac mechanics during sleep on Earth and in microgravity from the seismocardiogram”. In: *Scientific Reports* 7.1 (Nov. 15, 2017), p. 15634. ISSN: 2045-2322. DOI: 10.1038/s41598-017-15829-0. URL: https://www.nature.com/articles/s41598-017-15829-0 (visited on 03/21/2023).

[Don22] Shuqin Dong, Li Wen, Zhi Zhang, Changzhan Gu, and Junfa Mao. “Contactless Measurement of Human Systolic Time Intervals Based on Doppler Cardiograms in Clinical Environment”. In: *IEEE Microwave and Wireless Components Letters* 32.6 (June 2022), pp. 796–799. ISSN: 1558-1764. DOI: 10.1109/LMWC.2022.3157596.

[Dro22] L. Drost, J. B. Finke, J. Port, and H. Schächinger. “Comparison of TWA and PEP as indices of α2- and ß-adrenergic activation”. In: *Psychopharmacology* (Apr. 8, 2022). ISSN: 0033-3158, 1432-2072. DOI: 10.1007/s00213-022-06114-8. URL: https://link.springer.com/10.1007/s00213-022-06114-8 (visited on 05/13/2022).

[Ein08] Willem Einthoven. “Weiteres über das Elektrokardiogramm”. In: *Pflügers Archiv European Journal of Physiology* 122.12 (1908), pp. 517–584. URL: https://ia800708.us.archive.org/view_archive.php?archive=/22/items/crossref-pre-1909-scholarly-works/10.1007%252Fbf01677306.zip&file=10.1007%252Fbf01677829.pdf.

[Emp23] EmpkinS. *Website of the CRC 1483 EmpkinS*. 2023. URL: https://www.empkins.de/ (visited on 04/10/2023).

[Fer94] F. Ferraris, I. Gorini, U. Grimaldi, and M. Parvis. “Calibration of three-axial rate gyros without angular velocity standards”. In: *Sensors and Actuators A: Physical*. Proceedings of Eurosensors VIII 42.1 (Apr. 15, 1994), pp. 446–449. ISSN: 0924-4247. DOI: 10.1016/0924-4247(94)80031-6. URL: https://www.sciencedirect.com/science/article/pii/0924424794800316 (visited on 04/10/2023).

[Fol10] Paul Foley and Clemens Kirschbaum. “Human hypothalamus–pituitary–adrenal axis responses to acute psychosocial stress in laboratory settings”. In: *Neuroscience & Biobehavioral Reviews*. Psychophysiological Biomarkers of Health 35.1 (Sept. 1, 2010), pp. 91–96. ISSN: 0149-7634. DOI: 10.1016/j.neubiorev.

2010.01.010. URL: https://www.sciencedirect.com/science/article/pii/S0149763410000114 (visited on 01/20/2023).

[For18] Mohamad Forouzanfar, Fiona C. Baker, Massimiliano de Zambotti, Corey McCall, Laurent Giovangrandi, and Gregory T. A. Kovacs. "Toward a better noninvasive assessment of preejection period: A novel automatic algorithm for B-point detection and correction on thoracic impedance cardiogram". In: *Psychophysiology* 55.8 (Aug. 2018), e13072. ISSN: 00485772. DOI: 10.1111/psyp.13072. URL: https://onlinelibrary.wiley.com/doi/10.1111/psyp.13072 (visited on 11/15/2022).

[For19] Mohamad Forouzanfar, Fiona C. Baker, Ian M. Colrain, Aimée Goldstone, and Massimiliano Zambotti. "Automatic analysis of pre-ejection period during sleep using impedance cardiogram". In: *Psychophysiology* 56.7 (July 2019), e13355. ISSN: 0048-5772, 1469-8986. DOI: 10.1111/psyp.13355. URL: https://onlinelibrary.wiley.com/doi/10.1111/psyp.13355 (visited on 11/15/2022).

[Gra19] Stefan Gradl, Markus Wirth, Robert Richer, Nicolas Rohleder, and Bjoern M. Eskofier. "An Overview of the Feasibility of Permanent, Real-Time, Unobtrusive Stress Measurement with Current Wearables". In: *Proceedings of the 13th EAI International Conference on Pervasive Computing Technologies for Healthcare*. PervasiveHealth'19. New York, NY, USA: Association for Computing Machinery, May 20, 2019, pp. 360–365. ISBN: 978-1-4503-6126-2. DOI: 10.1145/3329189.3329233. URL: https://doi.org/10.1145/3329189.3329233 (visited on 03/03/2023).

[Ha20] Unsoo Ha, Salah Assana, and Fadel Adib. "Contactless seismocardiography via deep learning radars". In: *Proceedings of the 26th Annual International Conference on Mobile Computing and Networking*. MobiCom '20. New York, NY, USA: Association for Computing Machinery, Sept. 18, 2020, pp. 1–14. ISBN: 978-1-4503-7085-1. DOI: 10.1145/3372224.3419982. URL: https://doi.org/10.1145/3372224.3419982 (visited on 01/23/2023).

[Har67] Willard S. Harris, Clyde D. Schoenfeld, and Arnold M. Weissler. "Effects of Adrenergic Receptor Activation and Blockade on the Systolic Preejection Period, Heart Rate, and Arterial Pressure in Man". In: *The Journal of Clinical Investigation* 46.11 (Nov. 1, 1967), pp. 1704–1714. ISSN: 0021-9738. DOI: 10.

1172/JCI105661. URL: https://www.jci.org/articles/view/105661 (visited on 01/22/2023).

[Hea90] Martha E. Heath and John A. Downey. "The cold face test (diving reflex) in clinical autonomic assessment: methodological considerations and repeatability of responses". In: *Clinical Science* 78.2 (Feb. 1, 1990), pp. 139–147. ISSN: 0143-5221, 1470-8736. DOI: 10.1042/cs0780139. URL: https://portlandpress.com/clinsci/article/78/2/139/75178/The-cold-face-test-diving-reflex-in-clinical (visited on 04/04/2023).

[Hel12] Juliane Hellhammer and Melanie Schubert. "The physiological response to Trier Social Stress Test relates to subjective measures of stress during but not before or after the test". In: *Psychoneuroendocrinology* 37.1 (Jan. 1, 2012), pp. 119–124. ISSN: 0306-4530. DOI: 10.1016/j.psyneuen.2011.05.012. URL: https://www.sciencedirect.com/science/article/pii/S030645301100165X (visited on 04/17/2023).

[Her22] Liv Herzer, Annika Muecke, Robert Richer, Nils C. Albrecht, Markus Heyder, Katharina M. Jaeger, Veronika Koenig, Alexander Koelpin, Nicolas Rohleder, and Bjoern M. Eskofier. "Influence of Sensor Position and Body Movements on Radar-Based Heart Rate Monitoring". In: *2022 IEEE-EMBS International Conference on Biomedical and Health Informatics (BHI)*. 2022 IEEE-EMBS International Conference on Biomedical and Health Informatics (BHI). ISSN: 2641-3604. Sept. 2022, pp. 1–4. DOI: 10.1109/BHI56158.2022.9926775.

[Hos97] Y. Hoshikawa and Y. Yamamoto. "Effects of Stroop color-word conflict test on the autonomic nervous system responses". In: *American Journal of Physiology-Heart and Circulatory Physiology* 272.3 (Mar. 1, 1997), H1113–H1121. ISSN: 0363-6135, 1522-1539. DOI: 10.1152/ajpheart.1997.272.3.H1113. URL: https://www.physiology.org/doi/10.1152/ajpheart.1997.272.3.H1113 (visited on 04/03/2023).

[Hou05] Jan H. Houtveen, Paul F.C. Groot, and Eco J.C. Geus. "Effects of variation in posture and respiration on RSA and pre-ejection period". In: *Psychophysiology* 42.6 (Nov. 2005), pp. 713–719. ISSN: 0048-5772, 1469-8986. DOI: 10.1111/j.1469-8986.2005.00363.x. URL: https://onlinelibrary.wiley.com/doi/10.1111/j.1469-8986.2005.00363.x (visited on 04/29/2022).

[Jaf17] Mojtaba Jafari Tadi, Eero Lehtonen, Antti Saraste, Jarno Tuominen, Juho Koskinen, Mika Teräs, Juhani Airaksinen, Mikko Pänkäälä, and Tero Koivisto. "Gyrocardiography: A New Non-invasive Monitoring Method for the Assessment of Cardiac Mechanics and the Estimation of Hemodynamic Variables". In: *Scientific Reports* 7.1 (July 28, 2017), p. 6823. ISSN: 2045-2322. DOI: 10.1038/s41598-017-07248-y. URL: https://www.nature.com/articles/s41598-017-07248-y (visited on 03/21/2023).

[Jav16] Abdul Q. Javaid, Hazar Ashouri, and Omer T. Inan. "Estimating systolic time intervals during walking using wearable ballistocardiography". In: *2016 IEEE-EMBS International Conference on Biomedical and Health Informatics (BHI)*. 2016 IEEE-EMBS International Conference on Biomedical and Health Informatics (BHI). ISSN: 2168-2208. Feb. 2016, pp. 549–552. DOI: 10.1109/BHI.2016.7455956.

[Kaz79] Alan E. Kazdin. "Unobtrusive measures in behavioral assessment". In: *Journal of Applied Behavior Analysis* 12.4 (1979), pp. 713–724. ISSN: 00218855. DOI: 10.1901/jaba.1979.12-713. URL: http://doi.wiley.com/10.1901/jaba.1979.12-713 (visited on 03/03/2023).

[Keb20] Mamady Kebe, Rida Gadhafi, Baker Mohammad, Mihai Sanduleanu, Hani Saleh, and Mahmoud Al-Qutayri. "Human Vital Signs Detection Methods and Potential Using Radars: A Review". In: *Sensors* 20.5 (Jan. 2020), p. 1454. ISSN: 1424-8220. DOI: 10.3390/s20051454. URL: https://www.mdpi.com/1424-8220/20/5/1454 (visited on 01/24/2023).

[Khu06] Ramesh K. Khurana and Roger Wu. "The cold face test: A non-baroreflex mediated test of cardiac vagal function". In: *Clinical Autonomic Research* 16.3 (June 1, 2006), pp. 202–207. ISSN: 1619-1560. DOI: 10.1007/s10286-006-0332-9. URL: https://doi.org/10.1007/s10286-006-0332-9 (visited on 04/04/2023).

[Khu80] Ramesh K. Khurana, Sadakiyo Watabiki, J. R. Hebel, Rodrigo Toro, and Erland Nelson. "Cold face test in the assessment of trigeminal-brainstem- vagal function in humans". In: *Annals of Neurology* 7.2 (Feb. 1980), pp. 144–149. ISSN: 0364-5134, 1531-8249. DOI: 10.1002/ana.410070209. URL: https://onlinelibrary.wiley.com/doi/10.1002/ana.410070209 (visited on 04/03/2023).

[Kim18] Hye-Geum Kim, Eun-Jin Cheon, Dai-Seg Bai, Young Hwan Lee, and Bon-Hoon Koo. "Stress and Heart Rate Variability: A Meta-Analysis and Review of the Literature". In: *Psychiatry Investigation* 15.3 (Mar. 25, 2018). tex.ids= Kim2018, Kim2018b, kim2018stress publisher: Korean Neuropsychiatric Association, pp. 235–245. ISSN: 1738-3684. DOI: 10.30773/pi.2017.08.17. URL: http://psychiatryinvestigation.org/journal/view.php?doi=10.30773/pi.2017.08.17.

[Kir93] Clemens Kirschbaum, Karl-Martin Pirke, and Dirk H. Hellhammer. "The 'Trier Social Stress Test' – A Tool for Investigating Psychobiological Stress Responses in a Laboratory Setting". In: *Neuropsychobiology* 28.1 (1993), pp. 76–81. ISSN: 0302-282X, 1423-0224. DOI: 10.1159/000119004. URL: https://www.karger.com/Article/FullText/119004 (visited on 04/03/2023).

[Klu20] Michael Klum, Mike Urban, Timo Tigges, Alexandru-Gabriel Pielmus, Aarne Feldheiser, Theresa Schmitt, and Reinhold Orglmeister. "Wearable Cardiorespiratory Monitoring Employing a Multimodal Digital Patch Stethoscope: Estimation of ECG, PEP, LVET and Respiration Using a 55 mm Single-Lead ECG and Phonocardiogram". In: *Sensors* 20.7 (Jan. 2020), p. 2033. ISSN: 1424-8220. DOI: 10.3390/s20072033. URL: https://www.mdpi.com/1424-8220/20/7/2033 (visited on 01/27/2023).

[Koe14] S. Koegelenberg, C. Scheffer, M. M. Blanckenberg, and A. F. Doubell. "Application of Laser Doppler Vibrometery for human heart auscultation". In: *2014 36th Annual International Conference of the IEEE Engineering in Medicine and Biology Society*. 2014 36th Annual International Conference of the IEEE Engineering in Medicine and Biology Society. ISSN: 1558-4615. Aug. 2014, pp. 4479–4482. DOI: 10.1109/EMBC.2014.6944618.

[Kro17] J. Krohova, B. Czippelova, Z. Turianikova, Z. Lazarova, I. Tonhajzerova, and M. Javorka. "Preejection Period as a Sympathetic Activity Index: a Role of Confounding Factors". In: *Physiological Research* (Aug. 31, 2017), S265–S275. ISSN: 1802-9973, 0862-8408. DOI: 10.33549/physiolres.933682. URL: http://www.biomed.cas.cz/physiolres/pdf/2017/66_S265.pdf (visited on 03/27/2023).

[Kub70] W. G. Kubicek, R. P. Patterson, and D. A. Witsoe. “Impedance Cardiography as a Noninvasive Method of Monitoring Cardiac Function and Other Parameters of the Cardiovascular System”. In: *Annals of the New York Academy of Sciences* 170.2 (July 1970), pp. 724–732. ISSN: 0077-8923, 1749-6632. DOI: 10.1111/j.1749-6632.1970.tb17735.x. URL: https://onlinelibrary.wiley.com/doi/10.1111/j.1749-6632.1970.tb17735.x (visited on 11/15/2022).

[Küd22] Arne Küderle, Nils Roth, and Robert Richer. *imucal - a python library to calibrate 6 dof imus*. Version 2.3.1. 2022. URL: https://github.com/mad-lab-fau/imucal.

[Kum16] Puneet Kumar Jain and Anil Kumar Tiwari. “A novel method for suppression of motion artifacts from the seismocardiogram signal”. In: *2016 IEEE International Conference on Digital Signal Processing (DSP)*. 2016 IEEE International Conference on Digital Signal Processing (DSP). ISSN: 2165-3577. Oct. 2016, pp. 6–10. DOI: 10.1109/ICDSP.2016.7868504.

[Lab70] Zuhdi Lababidi, D. A. Ehmke, Robert E. Durnin, Paul E. Leaverton, and Ronald M. Lauer. “The First Derivative Thoracic Impedance Cardiogram”. In: *Circulation* 41.4 (Apr. 1970), pp. 651–658. ISSN: 0009-7322, 1524-4539. DOI: 10.1161/01.CIR.41.4.651. URL: https://www.ahajournals.org/doi/10.1161/01.CIR.41.4.651 (visited on 03/12/2023).

[Lea52] Aubrey Leatham. “Phonocardiography”. In: *British Medical Bulletin* 8.4 (1952), pp. 333–343. DOI: 10.1093/oxfordjournals.bmb.a074199.

[Lem15] Frédéric Lemaitre and Bernhard J. Schaller. “Chapter 15 - The Trigeminocardiac Reflex: A Comparison with the Diving Reflex in Humans”. In: *Trigeminocardiac Reflex*. Ed. by Tumul Chowdhury and Bernhard J. Schaller. Boston: Academic Press, Jan. 1, 2015, pp. 193–206. ISBN: 978-0-12-800421-0. DOI: 10.1016/B978-0-12-800421-0.00015-1. URL: https://www.sciencedirect.com/science/article/pii/B9780128004210000151 (visited on 04/03/2023).

[Lew77] R P Lewis, S E Rittogers, W F Froester, and H Boudoulas. “A critical review of the systolic time intervals.” In: *Circulation* 56.2 (Aug. 1977), pp. 146–158. ISSN: 0009-7322, 1524-4539. DOI: 10.1161/01.CIR.56.2.146. URL: https://www.ahajournals.org/doi/10.1161/01.CIR.56.2.146 (visited on 03/27/2023).

[Li21] Haobo Li, Ajay Mehul, Julien Le Kernec, Sevgi Z. Gurbuz, and Francesco Fioranelli. "Sequential Human Gait Classification With Distributed Radar Sensor Fusion". In: *IEEE Sensors Journal* 21.6 (Mar. 2021), pp. 7590–7603. ISSN: 1558-1748. DOI: 10.1109/JSEN.2020.3046991.

[Lie13] René van Lien, Nienke M. Schutte, Jan H. Meijer, and Eco J. C. de Geus. "Estimated preejection period (PEP) based on the detection of the R-wave and dZ/dt-min peaks does not adequately reflect the actual PEP across a wide range of laboratory and ambulatory conditions". In: *International Journal of Psychophysiology* 87.1 (Jan. 1, 2013), pp. 60–69. ISSN: 0167-8760. DOI: 10.1016/j.ijpsycho.2012.11.001. URL: https://www.sciencedirect.com/science/article/pii/S0167876012006460 (visited on 01/23/2023).

[Lin09] Peter Lindholm and Claes Eg Lundgren. "The physiology and pathophysiology of human breath-hold diving". In: *Journal of Applied Physiology* 106.1 (Jan. 2009), pp. 284–292. ISSN: 8750-7587, 1522-1601. DOI: 10.1152/japplphysiol.90991.2008. URL: https://www.physiology.org/doi/10.1152/japplphysiol.90991.2008 (visited on 04/03/2023).

[Lin15] Alexandra Linnemann, Beate Ditzen, Jana Strahler, Johanna M. Doerr, and Urs M. Nater. "Music listening as a means of stress reduction in daily life". In: *Psychoneuroendocrinology* 60 (Oct. 1, 2015), pp. 82–90. ISSN: 0306-4530. DOI: 10.1016/j.psyneuen.2015.06.008. URL: https://www.sciencedirect.com/science/article/pii/S0306453015002127 (visited on 04/03/2023).

[Lov75] William Lovallo. "The Cold Pressor Test and Autonomic Function: A Review and Integration". In: *Psychophysiology* 12.3 (May 1975), pp. 268–282. ISSN: 0048-5772, 1469-8986. DOI: 10.1111/j.1469-8986.1975.tb01289.x. URL: https://onlinelibrary.wiley.com/doi/10.1111/j.1469-8986.1975.tb01289.x (visited on 04/03/2023).

[Mai21] Julien Maitre, Kévin Bouchard, Camille Bertuglia, and Sébastien Gaboury. "Recognizing activities of daily living from UWB radars and deep learning". In: *Expert Systems with Applications* 164 (Feb. 1, 2021), p. 113994. ISSN: 0957-4174. DOI: 10.1016/j.eswa.2020.113994. URL: https://www.sciencedirect.com/science/article/pii/S0957417420307703 (visited on 01/24/2023).

[Mak21] Dominique Makowski, Tam Pham, Zen J. Lau, Jan C. Brammer, François Lespinasse, Hung Pham, Christopher Schölzel, and S. H. Annabel Chen. "NeuroKit2: A Python toolbox for neurophysiological signal processing". In: *Behavior Research Methods* 53.4 (Aug. 2021), pp. 1689–1696. ISSN: 1554-3528. DOI: 10.3758/s13428-020-01516-y. URL: https://link.springer.com/10.3758/s13428-020-01516-y (visited on 04/10/2023).

[Mar04] J.P. Martinez, R. Almeida, S. Olmos, A.P. Rocha, and P. Laguna. "A wavelet-based ECG delineator: evaluation on standard databases". In: *IEEE Transactions on Biomedical Engineering* 51.4 (Apr. 2004), pp. 570–581. ISSN: 1558-2531. DOI: 10.1109/TBME.2003.821031.

[Mar12] Manuel Martinez and Rainer Stiefelhagen. "Breath rate monitoring during sleep using near-ir imagery and PCA". In: *Proceedings of the 21st International Conference on Pattern Recognition (ICPR2012)*. Proceedings of the 21st International Conference on Pattern Recognition (ICPR2012). ISSN: 1051-4651. Nov. 2012, pp. 3472–3475.

[McC07] Laurie Kelly McCorry. "Physiology of the Autonomic Nervous System". In: *American Journal of Pharmaceutical Education* 71.4 (2007), p. 78. ISSN: 0002-9459. URL: https://www.ncbi.nlm.nih.gov/pmc/articles/PMC1959222/ (visited on 01/21/2023).

[McC16] R. McCarty. "The Fight-or-Flight Response: A Cornerstone of Stress Research". In: *Stress: Concepts, Cognition, Emotion, and Behavior*. Ed. by George Fink. San Diego: Academic Press, Jan. 1, 2016, pp. 33–37. ISBN: 978-0-12-800951-2. DOI: 10.1016/B978-0-12-800951-2.00004-2. URL: https://www.sciencedirect.com/science/article/pii/B9780128009512000042 (visited on 01/21/2023).

[Mic19] Fabian Michler, Kilin Shi, Sven Schellenberger, Tobias Steigleder, Anke Malessa, Laura Hameyer, Nina Neumann, Fabian Lurz, Christoph Ostgathe, Robert Weigel, and Alexander Koelpin. "A Clinically Evaluated Interferometric Continuous-Wave Radar System for the Contactless Measurement of Human Vital Parameters". In: *Sensors* 19.11 (Jan. 2019), p. 2492. ISSN: 1424-8220. DOI: 10.3390/s19112492. URL: https://www.mdpi.com/1424-8220/19/11/2492 (visited on 03/08/2023).

[Mil22] Nadica Miljković and Tomislav B. Šekara. *A New Weighted Time Window-based Method to Detect B-point in ICG*. July 10, 2022. DOI: 10.48550/arXiv.2207.04490. arXiv: 2207.04490[eess]. URL: http://arxiv.org/abs/2207.04490 (visited on 11/15/2022).

[Mil90] William R. Milnor. *Cardiovascular Physiology*. Google-Books-ID: 1duFI886FxIC. Oxford University Press, 1990. 526 pp. ISBN: 978-0-19-505884-0. URL: https://books.google.de/books?hl=de&lr=&id=1duFI886FxIC&oi=fnd&pg=PA3&dq=Cardiovascular+Physiology&ots=MSMhiGuIwL&sig=EuXvGgkGfL1MjW6rpo-EO0u_rM8#v=onepage&q=Cardiovascular%20Physiology&f=false.

[Mir21] Haroon Yousuf Mir and Omkar Singh. "ECG denoising and feature extraction techniques – a review". In: *Journal of Medical Engineering & Technology* 45.8 (Nov. 17, 2021), pp. 672–684. ISSN: 0309-1902. DOI: 10.1080/03091902.2021.1955032. URL: https://doi.org/10.1080/03091902.2021.1955032 (visited on 04/14/2023).

[Mor07] Umberto Morbiducci, Lorenzo Scalise, Mirko De Melis, and Mauro Grigioni. "Optical Vibrocardiography: A Novel Tool for the Optical Monitoring of Cardiac Activity". In: *Annals of Biomedical Engineering* 35.1 (Jan. 1, 2007), pp. 45–58. ISSN: 1573-9686. DOI: 10.1007/s10439-006-9202-9. URL: https://doi.org/10.1007/s10439-006-9202-9 (visited on 03/23/2023).

[Nat09] U. M. Nater and N. Rohleder. "Salivary alpha-amylase as a non-invasive biomarker for the sympathetic nervous system: Current state of research". In: *Psychoneuroendocrinology* 34.4 (May 1, 2009), pp. 486–496. ISSN: 0306-4530. DOI: 10.1016/j.psyneuen.2009.01.014. URL: https://www.sciencedirect.com/science/article/pii/S0306453009000328 (visited on 01/21/2023).

[New79] David B. Newlin and Robert W. Levenson. "Pre-ejection Period: Measuring Beta-adrenergic Influences Upon the Heart". In: *Psychophysiology* 16.6 (Nov. 1979), pp. 546–552. ISSN: 0048-5772, 1469-8986. DOI: 10.1111/j.1469-8986.1979.tb01519.x. URL: https://onlinelibrary.wiley.com/doi/10.1111/j.1469-8986.1979.tb01519.x (visited on 01/22/2023).

[Nou22] Muhammad Nouman, Sui Yang Khoo, M. A. Parvez Mahmud, and Abbas Z. Kouzani. "Recent Advances in Contactless Sensing Technologies for Mental Health Monitoring". In: *IEEE Internet of Things Journal* 9.1 (Jan. 2022), pp. 274–297. ISSN: 2327-4662. DOI: 10.1109/JIOT.2021.3097801.

[Oba17] Ezemenari M. Obasi, Elizabeth A. Shirtcliff, Lucia Cavanagh, Kristen L. Ratliff, Delishia M. Pittman, and Jessica J. Brooks. "Hypothalamic-Pituitary-Adrenal Reactivity to Acute Stress: an Investigation into the Roles of Perceived Stress and Family Resources". In: *Prevention Science* 18.8 (Nov. 1, 2017), pp. 923–931. ISSN: 1573-6695. DOI: 10.1007/s11121-017-0759-3. URL: https://doi.org/10.1007/s11121-017-0759-3 (visited on 04/17/2023).

[OCo21] Daryl B. O'Connor, Julian F. Thayer, and Kavita Vedhara. "Stress and Health: A Review of Psychobiological Processes". In: *Annual Review of Psychology* 72 (Jan. 4, 2021), pp. 663–688. ISSN: 1545-2085. DOI: 10.1146/annurev-psych-062520-122331.

[Opb18] Chantal J. M. van Opbergen, Stephanie M. van der Voorn, Marc A. Vos, Teun P. de Boer, and Toon A. B. van Veen. "Cardiac Ca2+ signalling in zebrafish: Translation of findings to man". In: *Progress in Biophysics and Molecular Biology*. The Use of Zebrafish for Cardiac Research 138 (Oct. 1, 2018), pp. 45–58. ISSN: 0079-6107. DOI: 10.1016/j.pbiomolbio.2018.05.002. URL: https://www.sciencedirect.com/science/article/pii/S0079610718300312 (visited on 03/25/2023).

[Opi04] Lionel H. Opie. *Heart Physiology: From Cell to Circulation*. Google-Books-ID: CPVSg69CPMsC. Lippincott Williams & Wilkins, 2004. 694 pp. ISBN: 978-0-7817-4278-8. URL: https://books.google.de/books?hl=de&lr=&id=CPVSg69CPMsC&oi=fnd&pg=PR9&dq=Heart+Physiology:+From+Cell+to+Circulation&ots=D2gMHqjdE_&sig=wP9Az6zzUNC7gA9R3GWzCff1S-o#v=onepage&q&f=false.

[Ott13] Catherine M. Otto. *Textbook of Clinical Echocardiography*. Elsevier Health Sciences, 2013. 572 pp. ISBN: 978-1-4557-2857-2.

[Pou20] Malikeh Pour Ebrahim, Fatemeh Heydari, Jean-Michel Redouté, and Mehmet Rasit Yuce. "Pre-Ejection Period (PEP) Estimation Based on R-Wave in ECG and On-Body Continuous Wave Radar Signal During Daily Activities". In: *13th EAI*

International Conference on Body Area Networks. EAI/Springer Innovations in Communication and Computing. Cham: Springer International Publishing, 2020, pp. 283–291. ISBN: 978-3-030-29897-5. DOI: 10.1007/978-3-030-29897-5_23.

[Rah18] Saif Rahman, Matthew Habel, and Richard J. Contrada. "Poincaré plot indices as measures of sympathetic cardiac regulation: Responses to psychological stress and associations with pre-ejection period". In: *International Journal of Psychophysiology* 133 (Nov. 2018), pp. 79–90. ISSN: 01678760. DOI: 10.1016/j.ijpsycho.2018.08.005. URL: https://linkinghub.elsevier.com/retrieve/pii/S0167876018300564 (visited on 04/29/2022).

[Rei04] Henrik Reims, Knut Sevre, Eigil Fossum, Aud Høieggen, Ivar Eide, and Sverre Kjeldsen. "Plasma catecholamines, blood pressure responses and perceived stress during mental arithmetic stress in young men". In: *Blood Pressure* 13.5 (Jan. 1, 2004), pp. 287–294. ISSN: 0803-7051. DOI: 10.1080/08037050410016474. URL: https://doi.org/10.1080/08037050410016474 (visited on 04/03/2023).

[Rey13] Gustavo A. Reyes del Paso, Wolf Langewitz, Lambertus J. M. Mulder, Arie van Roon, and Stefan Duschek. "The utility of low frequency heart rate variability as an index of sympathetic cardiac tone: A review with emphasis on a reanalysis of previous studies: LF HRV and sympathetic cardiac tone". In: *Psychophysiology* 50.5 (May 2013), pp. 477–487. ISSN: 00485772. DOI: 10.1111/psyp.12027. URL: https://onlinelibrary.wiley.com/doi/10.1111/psyp.12027 (visited on 01/22/2023).

[Ric21] Robert Richer, Arne Küderle, Martin Ullrich, Nicolas Rohleder, and Bjoern Eskofier. "BioPsyKit: A Python package for the analysis of biopsychological data". In: *Journal of Open Source Software* 6.66 (Oct. 12, 2021), p. 3702. ISSN: 2475-9066. DOI: 10.21105/joss.03702. URL: https://joss.theoj.org/papers/10.21105/joss.03702 (visited on 04/10/2023).

[Ric22] Robert Richer, Janis Zenkner, Arne Küderle, Nicolas Rohleder, and Bjoern M. Eskofier. "Vagus activation by Cold Face Test reduces acute psychosocial stress responses". In: *Scientific Reports* 12.1 (Nov. 10, 2022), p. 19270. ISSN: 2045-2322. DOI: 10.1038/s41598-022-23222-9. URL: https://www.nature.com/articles/s41598-022-23222-9 (visited on 04/03/2023).

[Ric23] Robert Richer, Victoria Mueller, Arne Kuederle, Nicolas Rohleder, and Bjoern M Eskofier. "stress+ - Towards an Open-Source Web Application for the Remote Induction of Acute Psychosocial Stress". In: *Psychosomatic Medicine*. LIPPINCOTT WILLIAMS & WILKINS TWO COMMERCE SQ, 2001 MARKET ST, PHILADELPHIA, 2023.

[Rot18] Nils Roth, Christine F. Martindale, Bjoern M. Eskofier, Heiko Gaßner, Zacharias Kohl, and Jochen Klucken. "Synchronized Sensor Insoles for Clinical Gait Analysis in Home-Monitoring Applications". In: *Current Directions in Biomedical Engineering* 4.1 (Sept. 1, 2018), pp. 433–437. ISSN: 2364-5504. DOI: 10.1515/cdbme-2018-0103. URL: https://www.degruyter.com/document/doi/10.1515/cdbme-2018-0103/html (visited on 04/09/2023).

[Rus19] Georgina Russell and Stafford Lightman. "The human stress response". In: *Nature Reviews Endocrinology* 15.9 (Sept. 2019), pp. 525–534. ISSN: 1759-5037. DOI: 10.1038/s41574-019-0228-0. URL: https://www.nature.com/articles/s41574-019-0228-0 (visited on 01/20/2023).

[San20] Richard H. Sandler, Md Khushidul Azad, John D'Angelo, Peshala Gamage, Nirav Y. Raval, Robert J. Mentz, and Hansen A. Mansy. "Documenting Spatial Variation of SCG Signals for Optimal Sensor Placement". In: *Journal of Cardiac Failure*. Abstracts From the Heart Failure Society of America's (HFSA) Annual Scientific Meeting 2020 26.10 (Oct. 1, 2020), S92. ISSN: 1071-9164. DOI: 10.1016/j.cardfail.2020.09.269. URL: https://www.sciencedirect.com/science/article/pii/S1071916420312161 (visited on 04/16/2023).

[San22] Francesca Santucci, Daniela Lo Presti, Carlo Massaroni, Emiliano Schena, and Roberto Setola. "Precordial Vibrations: A Review of Wearable Systems, Signal Processing Techniques, and Main Applications". In: *Sensors* 22.15 (Jan. 2022), p. 5805. ISSN: 1424-8220. DOI: 10.3390/s22155805. URL: https://www.mdpi.com/1424-8220/22/15/5805 (visited on 01/27/2023).

[Sch83] Peter J. Schwartz and Theodore Weiss. "T-Wave Amplitude as an Index of Cardiac Sympathetic Activity: A Misleading Concept". In: *Psychophysiology* 20.6 (Nov. 1983), pp. 696–701. ISSN: 0048-5772. DOI: 10.1111/j.1469-8986.1983.tb00941.x. URL: http://doi.wiley.com/10.1111/j.1469-8986.1983.tb00941.x.

[Sei21] Ann-Kathrin Seifert, Martin Grimmer, and Abdelhak M. Zoubir. "Doppler Radar for the Extraction of Biomechanical Parameters in Gait Analysis". In: *IEEE Journal of Biomedical and Health Informatics* 25.2 (Feb. 2021), pp. 547–558. ISSN: 2168-2208. DOI: 10.1109/JBHI.2020.2994471.

[Sha19] Md Mobashir Hasan Shandhi, Beren Semiz, Sinan Hersek, Nazli Goller, Farrokh Ayazi, and Omer T. Inan. "Performance Analysis of Gyroscope and Accelerometer Sensors for Seismocardiography-Based Wearable Pre-Ejection Period Estimation". In: *IEEE Journal of Biomedical and Health Informatics* PP (c 2019). Publisher: IEEE, pp. 1–1. ISSN: 2168-2194. DOI: 10.1109/JBHI.2019.2895775. URL: https://ieeexplore.ieee.org/document/8627923/.

[She90] Andrew Sherwood, Michael T. Allen, Jochen Fahrenberg, Robert M. Kelsey, William R. Lovallo, and Lorenz J.P. Doornen. "Methodological Guidelines for Impedance Cardiography". In: *Psychophysiology* 27.1 (Jan. 1990), pp. 1–23. ISSN: 0048-5772, 1469-8986. DOI: 10.1111/j.1469-8986.1990.tb02171.x. URL: https://onlinelibrary.wiley.com/doi/10.1111/j.1469-8986.1990.tb02171.x (visited on 01/22/2023).

[Shi18] Kilin Shi, Christoph Will, Tobias Steigleder, Fabian Michler, Robert Weigel, Christoph Ostgathe, and Alexander Koelpin. "A contactless system for continuous vital sign monitoring in palliative and intensive care". In: *2018 Annual IEEE International Systems Conference (SysCon)*. 2018 Annual IEEE International Systems Conference (SysCon). ISSN: 2472-9647. Apr. 2018, pp. 1–8. DOI: 10.1109/SYSCON.2018.8369507.

[Shi21] Kilin Shi, Tobias Steigleder, Sven Schellenberger, Fabian Michler, Anke Malessa, Fabian Lurz, Nicolas Rohleder, Christoph Ostgathe, Robert Weigel, and Alexander Koelpin. "Contactless analysis of heart rate variability during cold pressor test using radar interferometry and bidirectional LSTM networks". In: *Scientific Reports* 11.1 (Dec. 2021), p. 3025. ISSN: 2045-2322. DOI: 10.1038/s41598-021-81101-1. URL: http://www.nature.com/articles/s41598-021-81101-1 (visited on 03/24/2021).

[Sør18] Kasper Sørensen, Samuel E. Schmidt, Ask S. Jensen, Peter Søgaard, and Johannes J. Struijk. "Definition of Fiducial Points in the Normal Seismocardiogram". In: *Scientific Reports* 8.1 (Oct. 18, 2018), p. 15455. ISSN: 2045-2322. DOI: 10.1038/

s41598-018-33675-6. URL: https://www.nature.com/articles/s41598-018-33675-6 (visited on 03/31/2023).

[Sto10] Gijsbert Stoet. "PsyToolkit: A software package for programming psychological experiments using Linux". In: *Behavior Research Methods* 42.4 (Nov. 1, 2010), pp. 1096–1104. ISSN: 1554-3528. DOI: 10.3758/BRM.42.4.1096. URL: https://doi.org/10.3758/BRM.42.4.1096 (visited on 04/04/2023).

[Sto17] Gijsbert Stoet. "PsyToolkit: A Novel Web-Based Method for Running Online Questionnaires and Reaction-Time Experiments". In: *Teaching of Psychology* 44.1 (Jan. 2017), pp. 24–31. ISSN: 0098-6283, 1532-8023. DOI: 10.1177/0098628316677643. URL: http://journals.sagepub.com/doi/10.1177/0098628316677643 (visited on 04/04/2023).

[Str35] John R. Stroop. "Studies of interference in serial verbal reactions". In: *Journal of Experimental Psychology* 18.6 (1935), pp. 643–662. ISSN: 0022-1015. DOI: 10.1037/h0054651. URL: https://pure.mpg.de/rest/items/item_2389918/component/file_2389917/content (visited on 04/03/2023).

[Tak04] Noriyasu Takai, Masaki Yamaguchi, Toshiaki Aragaki, Kenji Eto, Kenji Uchihashi, and Yasuo Nishikawa. "Effect of psychological stress on the salivary cortisol and amylase levels in healthy young adults". In: *Archives of Oral Biology* 49.12 (Dec. 1, 2004), pp. 963–968. ISSN: 0003-9969. DOI: 10.1016/j.archoralbio.2004.06.007. URL: https://www.sciencedirect.com/science/article/pii/S0003996904001499 (visited on 04/03/2023).

[Tan15] Bo Tan, Alison Burrows, Robert Piechocki, Ian Craddock, Qingchao Chen, Karl Woodbridge, and Kevin Chetty. "Wi-Fi based passive human motion sensing for in-home healthcare applications". In: *2015 IEEE 2nd World Forum on Internet of Things (WF-IoT)*. 2015 IEEE 2nd World Forum on Internet of Things (WF-IoT). Dec. 2015, pp. 609–614. DOI: 10.1109/WF-IoT.2015.7389123.

[Tav10] Kouhyar Tavakolian, Andrew P. Blaber, Brandon Ngai, and Bozena Kaminska. "Estimation of hemodynamic parameters from seismocardiogram". In: *2010 Computing in Cardiology*. 2010 Computing in Cardiology. ISSN: 2325-8853. Sept. 2010, pp. 1055–1058. URL: https://ieeexplore.ieee.org/abstract/document/5738158.

[Tav16] Kouhyar Tavakolian. "Systolic Time Intervals and New Measurement Methods". In: *Cardiovascular Engineering and Technology* 7.2 (June 1, 2016), pp. 118–125. ISSN: 1869-4098. DOI: 10.1007/s13239-016-0262-1. URL: https://doi.org/10.1007/s13239-016-0262-1 (visited on 01/22/2023).

[The23] Eleni Theodoridou, Luigi Cinque, Filippo Mignosi, Giuseppe Placidi, Matteo Polsinelli, João Manuel R. S. Tavares, and Matteo Spezialetti. "Hand Tracking and Gesture Recognition by Multiple Contactless Sensors: A Survey". In: *IEEE Transactions on Human-Machine Systems* 53.1 (Feb. 2023), pp. 35–43. ISSN: 2168-2305. DOI: 10.1109/THMS.2022.3188840.

[Tho12] Myriam V. Thoma, Clemens Kirschbaum, Jutta M. Wolf, and Nicolas Rohleder. "Acute stress responses in salivary alpha-amylase predict increases of plasma norepinephrine". In: *Biological Psychology* 91.3 (Dec. 1, 2012), pp. 342–348. ISSN: 0301-0511. DOI: 10.1016/j.biopsycho.2012.07.008. URL: https://www.sciencedirect.com/science/article/pii/S0301051112001688 (visited on 01/20/2023).

[Tho19] Bianca Lee Thomas, Nicolaas Claassen, Piet Becker, and Margaretha Viljoen. "Validity of Commonly Used Heart Rate Variability Markers of Autonomic Nervous System Function". In: *Neuropsychobiology* 78.1 (2019), pp. 14–26. ISSN: 0302-282X, 1423-0224. DOI: 10.1159/000495519. URL: https://www.karger.com/Article/FullText/495519 (visited on 01/22/2023).

[Tul89] J. H. M. Tulen, P. Moleman, H. G. van Steenis, and F. Boomsma. "Characterization of stress reactions to the Stroop Color Word Test". In: *Pharmacology Biochemistry and Behavior* 32.1 (Jan. 1, 1989), pp. 9–15. ISSN: 0091-3057. DOI: 10.1016/0091-3057(89)90204-9. URL: https://www.sciencedirect.com/science/article/pii/0091305789902049 (visited on 04/04/2023).

[Ulr09] Yvonne M. Ulrich-Lai and James P. Herman. "Neural regulation of endocrine and autonomic stress responses". In: *Nature Reviews Neuroscience* 10.6 (June 2009), pp. 397–409. ISSN: 1471-0048. DOI: 10.1038/nrn2647. URL: https://www.nature.com/articles/nrn2647 (visited on 01/20/2023).

[Vel97] Manuel Velasco, Juanita Gómez, Mario Blanco, and Imelda Rodriguez. "THE COLD PRESSOR TEST: PHARMACOLOGICAL AND THERAPEUTIC AS-

PECTS". In: *American Journal of Therapeutics* 4.1 (Jan. 1997), p. 34. ISSN: 1075-2765. URL: https://journals.lww.com/americantherapeutics/Abstract/1997/01000/The_Cold_Pressor_Test__Pharmacological_and.8.aspx (visited on 04/04/2023).

[Wan19] Anran Wang, Jacob E. Sunshine, and Shyamnath Gollakota. "Contactless Infant Monitoring using White Noise". In: *The 25th Annual International Conference on Mobile Computing and Networking*. MobiCom '19. New York, NY, USA: Association for Computing Machinery, Oct. 11, 2019, pp. 1–16. ISBN: 978-1-4503-6169-9. DOI: 10.1145/3300061.3345453. URL: https://doi.org/10.1145/3300061.3345453 (visited on 01/23/2023).

[War83] Marcia M. Ward, Ivan N. Mefford, Stanley D. Parker, Margaret A. Chesney, Barr C. Taylor, David L. Keegan, and Jack D. Barchas. "Epinephrine and Norepinephrine Responses in Continuously Collected Human Plasma to a Series of Stressors". In: *Psychosomatic Medicine* 45.6 (Dec. 1983), p. 471. ISSN: 0033-3174. URL: https://journals.lww.com/psychosomaticmedicine/Citation/1983/12000/Epinephrine_and_Norepinephrine_Responses_in.2.aspx (visited on 04/04/2023).

[Wei21] David G Weissman. "Correlation of sympathetic and parasympathetic nervous system activity during rest and acute stress tasks". In: *International Journal of Psychophysiology* (2021), p. 9. URL: https://www.sciencedirect.com/science/article/abs/pii/S016787602100026X.

[Wei77] Arnold M. Weissler. "Systolic-Time Intervals". In: *New England Journal of Medicine* 296.6 (Feb. 10, 1977), pp. 321–324. ISSN: 0028-4793, 1533-4406. DOI: 10.1056/NEJM197702102960607. URL: http://www.nejm.org/doi/abs/10.1056/NEJM197702102960607 (visited on 01/22/2023).

[Wil18] Christoph Will, Kilin Shi, Sven Schellenberger, Tobias Steigleder, Fabian Michler, Jonas Fuchs, Robert Weigel, Christoph Ostgathe, and Alexander Koelpin. "Radar-Based Heart Sound Detection". In: *Scientific Reports* 8.1 (July 26, 2018), p. 11551. ISSN: 2045-2322. DOI: 10.1038/s41598-018-29984-5. URL: https://www.nature.com/articles/s41598-018-29984-5 (visited on 01/24/2023).

[Wol97] H H Woltjer, H J Bogaard, and P M J M De Vries. “The technique of impedance cardiography: A review”. In: *European heart journal* 18 (1997), pp. 1396–1403. URL: https://research.vumc.nl/ws/files/10004011/114097.

[Xia18] Zongyang Xia, Md. Mobashir Hasan Shandhi, Omer T. Inan, and Ying Zhang. “Non-Contact Sensing of Seismocardiogram Signals Using Microwave Doppler Radar”. In: *IEEE Sensors Journal* 18.14 (July 2018), pp. 5956–5964. ISSN: 1558-1748. DOI: 10.1109/JSEN.2018.2842122.

[Yan22] Yuzhe Yang, Yuan Yuan, Guo Zhang, Hao Wang, Ying-Cong Chen, Yingcheng Liu, Christopher G. Tarolli, Daniel Crepeau, Jan Bukartyk, Mithri R. Junna, Aleksandar Videnovic, Terry D. Ellis, Melissa C. Lipford, Ray Dorsey, and Dina Katabi. “Artificial intelligence-enabled detection and assessment of Parkinson’s disease using nocturnal breathing signals”. In: *Nature Medicine* 28.10 (Oct. 2022), pp. 2207–2215. ISSN: 1546-170X. DOI: 10.1038/s41591-022-01932-x. URL: https://www.nature.com/articles/s41591-022-01932-x (visited on 04/03/2023).

[Yue20] Shichao Yue, Yuzhe Yang, Hao Wang, Hariharan Rahul, and Dina Katabi. “BodyCompass: Monitoring Sleep Posture with Wireless Signals”. In: *Proceedings of the ACM on Interactive, Mobile, Wearable and Ubiquitous Technologies* 4.2 (June 15, 2020), 66:1–66:25. DOI: 10.1145/3397311. URL: https://doi.org/10.1145/3397311 (visited on 01/24/2023).

[Zan13] John M. Zanetti and Kouhyar Tavakolian. “Seismocardiography: Past, present and future”. In: *2013 35th Annual International Conference of the IEEE Engineering in Medicine and Biology Society (EMBC)*. 2013 35th Annual International Conference of the IEEE Engineering in Medicine and Biology Society (EMBC). ISSN: 1558-4615. July 2013, pp. 7004–7007. DOI: 10.1109/EMBC.2013.6611170.